University of Warsaw
Faculty of Physics

Katarzyna Frankiewicz
Student's book no.: 278502

Search for Dark Matter Particles with the Super-Kamiokande Detector

Second cycle degree thesis
field of study Physics
speciality Physics of elementary particles and fundamental interactions

The thesis written under the supervision of
dr Katarzyna Grzelak
Institute of Experimental Physics
Faculty of Physics, University of Warsaw
dr Piotr Mijakowski
National Centre for Nuclear Research

Warsaw, September 2013

Oświadczenie kierującego pracą

Oświadczam, że niniejsza praca została przygotowana pod moim kierunkiem i stwierdzam, że spełnia ona warunki do przedstawienia jej w postępowaniu o nadanie tytułu zawodowego.

Data Podpis kierującego pracą Data Podpis kierującego pracą

Statement of the Supervisor on Submission of the Thesis

I hereby certify that the thesis submitted has been prepared under my supervision and I declare that it satisfies the requirements of submission in the proceedings for the award of a degree.

Date Signature of the Supervisor Date Signature of the Supervisor

Oświadczenie autora pracy

Świadom odpowiedzialności prawnej oświadczam, że niniejsza praca dyplomowa została napisana przeze mnie samodzielnie i nie zawiera treści uzyskanych w sposób niezgodny z obowiązującymi przepisami.

Oświadczam również, że przedstawiona praca nie była wcześniej przedmiotem procedur związanych z uzyskaniem tytułu zawodowego w wyższej uczelni.

Oświadczam ponadto, że niniejsza wersja pracy jest identyczna z załączoną wersją elektroniczną.

Data Podpis autora pracy

Statement of the Author on Submission of the Thesis

Aware of legal liability I certify that the thesis submitted has been prepared by myself and does not include information gathered contrary to the law.

I also declare that the thesis submitted has not been the subject of proceedings resulting in the award of a university degree.

Furthermore I certify that the submitted version of the thesis is identical with its attached electronic version.

Date Signature of the Author of the thesis

Summary

W pracy przedstawiono analizę poszukiwania neutrin związanych z anihilacją Ciemnej Materii w Galaktyce przy wykorzystaniu danych zebranych w latach 1996-2008 przez detektor Super-Kamiokande. Przeprowadzone studia koncentrują się na poszukiwaniu nadwyżki przypadków neutrin pochodzących z kierunku centrum Galaktyki, gdzie przewidywana jest bardzo wysoka koncentracja cząstek Ciemnej Materii. Po przeanalizowaniu zebranych danych nie stwierdzono nadwyżki w obserwowanej liczbie neutrin z kierunku centrum Galaktyki w stosunku do obserwowanych przypadków oddziaływań neutrin atmosferycznych. Na tej podstawie wyznaczono górne granice dla wartości przekroju czynnego na anihilację dla cząstek ciemnej materii o masach z przedziału od 300 MeV do 10 TeV, dla trzech rozważanych modeli halo galaktycznego.

Key words

Ciemna Materia, metody detekcji Ciemnej Materii, neutrina, detektor Super-Kamiokande

Area of study (codes according to Erasmus Subject Area Codes List)

13.2 Physics

The title of the thesis in Polish

Poszukiwanie cząstek Ciemnej Materii w eksperymencie Super-Kamiokande

Abstract

This thesis presents a search for dark matter induced neutrinos in our Galaxy using data collected with the Super-Kamiokande detector in years 1996-2008. Dark matter density is expected to be largely enhanced in the area of the Galactic Center which may result in increased annihilation of a relic particles in that region. The analysis focuses on the search for angular anisotropy in the number of observed neutrino events between the Galactic Center and other parts of the sky where the expected flux of dark matter annihilation products is low. No excess of neutrinos from the Galactic Center region has been observed and the observed neutrino fluxes were consistent with the atmospheric neutrino background. Upper limits on the self-annihilation cross-section are obtained for dark matter particle masses ranging from 300 MeV to 10 TeV for various dark matter halo models.

Acknowledgments

First of all, I am heartily thankful to my supervisors, dr Piotr Mijakowski and dr Katarzyna Grzelak, who had supported me from the initial to the final level. I do feel that without long lasting discussions with Piotr and his great commitment this thesis would never come into existence.

I would like to extend my gratitude to prof. Ewa Rondio, who not only provided me with the opportunity to broaden my outlook, but also advised me on my research path. Thanks to the help of both Ewa and Piotr's I was able to visit Japan and present these results on Super-Kamiokande Collaboration Meeting, for which I am extremly grateful. Moreover, I would like to acknowledge dr Roman Nowak for his guidance and support with the statistical analysis.

This thesis would not have been possible without their patience, encouragement and guidance. My greatest debt is to my family and friends for their love and understanding.

Contents

Chapter 1

Introduction

Detection and elucidating the nature of a dark matter (DM) is one of the main goals of the astrophysics and particle physics nowadays. Dark matter neither emits nor absorbs light or other electromagnetic radiation and cannot be observed directly with telescopes. However, its existence and properties can be inferred from its gravitational effects on visible matter, radiation, and on the large-scale structure of the Universe. According to study of cosmic microwave background and based on standard cosmology model, dark matter is expected to account for a large part of the total mass in the Universe.

Various hypothesis regarding the nature of the dark matter has been proposed. Most of them suggest composition of new type, non-baryonic particles, and their production mechanisms going beyond the Standard Model. The most widely accepted proposal is that dark matter consist of non relativistic, neutral, long-lived Weakly Interacting Massive Particles (WIMPs). It is expected that WIMPs are present in the whole Universe forming large invisible structures which encompass visible matter formations[1].

There are two main strategies for dark matter detection - direct and indirect. The direct methods are based on the assumption that WIMPs can be elastically scattered on the baryonic nuclei. Many experiments attempt to measure the kinetic energy of resulting nuclear recoils. Current results are inconsistent and controversial (see Chapter 3). The other, indirect method, focuses on a search for products of dark matter self-annihilation, such as antimatter, photons or neutrinos. Alternatively to those methods, there are attempts to produce dark matter particles in the high energy particle accelerators like Large Hadron Collider (LHC).

This thesis presents the search for dark matter induced neutrinos based on a data collected with the Super-Kamiokande (SK) detector in years 1996-2008. The conducted analysis focuses on a search from the region of the Galactic Center, using atmospheric muon neutrinos. In Chapter 2, an overview of the dark matter concept is presented. The observational evidence of dark matter existence and possible candidates for dark matter particles are considered. Methodology of dark matter searches and current experimental results are discussed in Chapter 3. Super-Kamiokande detector description and principle of its operation are the subject of Chapter 4. Chapter 5 describes three different Milky Way halo models investigated in the analysis. The calculation of the spectrum of dark matter annihilation products is also presented there. The simulation of DM-induced neutrinos, which was developed for the purpose of this

analysis is discussed in Chapter 6. This chapter contains also description of analysed data and the concept of performed analysis. The results and upper limits on the self-annihilation cross-section obtained for dark matter particle masses ranging from 300 MeV to 10 TeV are presented in Chapter 7. The last chapter contains summary and outlook.

Chapter 2

Dark Matter

2.1 Observational Evidence

There are many compelling evidence indicating the presence of dark matter in the Universe[1]. They can be obtained at very different scales, from cosmological ones, through the analysis of the angular anisotropies in the cosmic microwave background radiation, down to galactic scales, considering gravitational lensing and dynamics of galaxies. First such an observation was made by Fritz Zwicky in 1933[2]. He had measured dynamics of galaxies in the Coma cluster. A total mass contained in the cluster, estimated from the emitted light, was not enough to explain observed high rotational velocities. Calculations had shown that there must be another component, which was called the dark matter. Similar observations in the Virgo cluster, were held by Sinclair Smith in the Mount Wilson Observatory in 1936[3]. He had came to the same conclusion as Zwicky.

The distributions of rotational velocities of stars in the galaxies are another evidence which supports the dark matter existence hypothesis. This type of observations were made by Vera Rubin's group in the 70s and 80s of the XX century[4]. Rotational velocities of the stars measured at different distances from the galactic center did not agree with the theoretical predictions based on visible matter distribution. Especially, the stars in outer region of the galaxy move faster than expected. This lead to the conclusion that there has to be additional invisible mass, which creates large structures placed even far beyond the visible edges of galaxies. Dark matter is the widely accepted explanation for this observations, however, numerous alternatives also have been proposed. Most of them postulate to modify the law of gravity, replacing the laws established by Newton and Einstein. These theories can be referred to as MOND[5].

Dark mater existence can be also inferred from observations of gravitational lensing. Light's trajectory is bended when it passes through a strong gravitational field. When the source of light is behind a massive invisible object, the image of the background source can be magnify and distort. Based on this effect, the total mass in the investigated region can be estimated. As an example among many, such observations were held for Bullet Cluster in August 2006[6]. A collision between two galaxy clusters caused a separation of dark and baryonic matter components. Electromagnetic interactions between passing gas particles caused them to slow down and as X-ray observations show, much of the baryonic matter is concentrated in the center, near the point of impact. On the other hand, gravitational lensing observations show that much of

the mass resides outside of the central region due to dark matter components of the two clusters, which passed through each other without slowing down substantially. Unlike the galactic rotation curves, this evidence for dark matter existence cannot be explained by the modification of laws of gravity.

Measurements of the cosmic microwave background (CMB) radiation allow for estimation of the total mass and energy amount in the Universe. WMAP's measurements played the key role in establishing of the current Standard Model of Cosmology, namely the ΛCDM model, which implies a flat Universe dominated by dark energy, supplemented by dark matter and baryonic matter[7]. The latest results obtained by Planck mission team implies that total mass-energy of the Universe contains 4.9% ordinary matter, 26.8% dark matter and 68.3% dark energy[8]. Dark matter seems to be essential in evolution of the Universe. Its presence is required in cosmological models of the Big Bang. Significant amount of nonbaryonic, cold dark matter is necessary to explain the large-scale structure formation of the Universe[9].

2.2 Dark Matter Candidates

Despite many proofs for the existence of dark matter, its nature is still unknown. At first, non-luminous heavy barionic objects, such as black holes, neutron stars, brown dwarfs, collectively named as massive compact halo objects (MACHO), were considered a possible candidate for dark matter. However, astronomical surveys for gravitational microlensing, including the MACHO, EROS and OGLE projects, along with Hubble telescope searches for ultra-faint stars, have not found enough of MACHOs and indicated that they could constitute only a very small portion of dark matter[10]. Standard Model does not provide viable non-baryonic candidates for dark matter particles and the existence of dark matter is one of the most compelling evidence for physics beyond the Standard Model.

One can distinguish two possible creation mechanisms among the dark matter candidates, thermal creation in the early Universe and non-thermal creation in a phase transition. In the early Universe the thermal equilibrium was obtained, so in case of particles which are created thermally, their number density was roughly equal to the number density of photons. Then, as the Universe cooled, the number of dark matter particles would decrease until the temperature of Universe finally dropped below the DM particle mass. At this point their creation would require being on the tail of the thermal distribution, number density would drop exponentially and the probability of pair annihilation would become small. The number density would "freeze-out" and left a substantial number of dark matter particles today $\Omega_{WIMP} \approx \frac{10^{-26} cm^3 s^{-1}}{<\sigma v>}$, where $<\sigma v>$ is the thermally averaged cross section for WIMPS annihilation into Standard Model particles.

Dark matter particle must be stable or long-lived, as it had been produced after the Big Bang and is still present today. Dark matter is required to be dynamically cold (not relativistic) so that it can clump and form gravitationally bound structures. The neutral particles which would be able to fulfill the above criteria and reproduce required dark matter density in the Universe derived from CMB measurements, additionally having a mass of the order of the electroweak scale belong to a group referred to as Weakly Interacting Massive Particles (WIMPs). Presently

WIMPs, with mass in the range from several GeV to few TeV are considered the best motivated dark matter candidate supported by Supersymmetry theories (SUSY), which provide one of the most popular WIMP candidate: the lightest supersymmetric particle (LSP), namely neutralino χ[11].

WIMPs are not the only candidate considered. Since it has been proved that neutrinos have mass and are abundant in the Universe, they were considered a good candidate. However, neutrinos can only form a small fraction of the dark matter, due to limits from a large-scale structure formation models and high-redshift galaxies observations. The most popular candidate beside WIMPs, is called axion and arise from attempts to explain why the strong interaction seems to obey a CP symmetry. The axions are stable and they can be also produced in the early Universe[12]. Although axions are expected to be far lighter than WIMPs (less than 1eV), they could be created in the right amount by a non-thermal processes which also naturally leaves them slow-moving. Many theorists suggest also that our Universe may have more spatial dimensions. If standard model particles propagate in extra dimensions, the lightest Kaluza-Klein state would be a good dark matter candidate[13]. In addition to the mainstream candidates described above, many more exotic candidates have been suggested, such as WIMPzillas, Q-balls and gravitinos.

Chapter 3

Search for Dark Matter

Weakly Interacting Massive Particle as dark matter candidate is a well posed scientific hypothesis and a subject of experimental verification. Numerous experiments attempt to detect dark matter using different methods and a wide variety of techniques. The experiments can be divided into two categories: direct detection experiments, which search for the scattering of dark matter particles off atomic nuclei, and indirect detection, which search for the products of WIMPs annihilations. An alternative approach to the detection of WIMPs is their production in the laboratory in very high energy collisions.

3.1 Direct detection

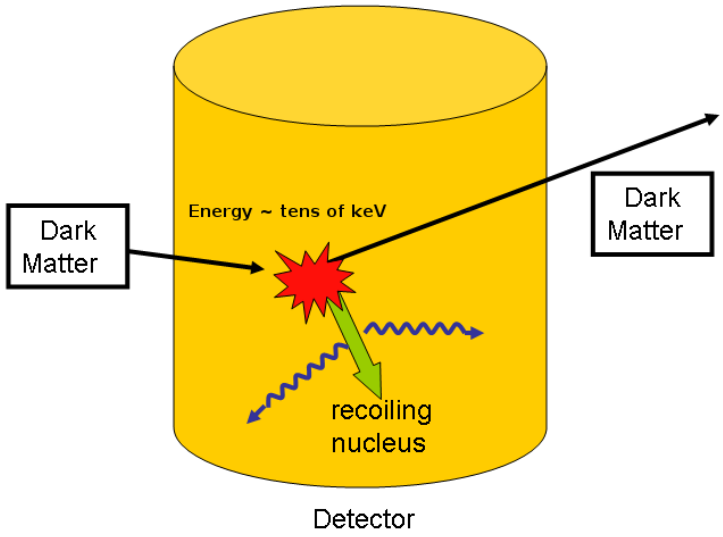

Figure 3.1: A sketch of dark matter direct detection idea.

It is expected that dark matter local density in the Galaxy at the Solar System position is 0.3 GeV/cm^3[14]. That implies that thousands of dark matter particles must pass through every square centimeter of the Earth in each second. In direct detection method one tries to detect the nuclear recoils originated by the rare interactions of the dark matter particles with the target nuclei (see Fig 3.1). The expected energy of nuclear recoils is in the range from several to

hundreds of keV depending on the mass of dark matter particle and type of the detector. In this energy range the main contribution to the experimental background comes from interactions of α-particles, neutrons, electrons, and photons on the detector target material. These backgrounds originate from decays of radioactive isotopes present in the materials surrounding the detectors, in airborne contaminants, or from within the detectors themselves. Therefore, appropriate shielding with passive and active materials as well as veto detectors around the experiment are very important.

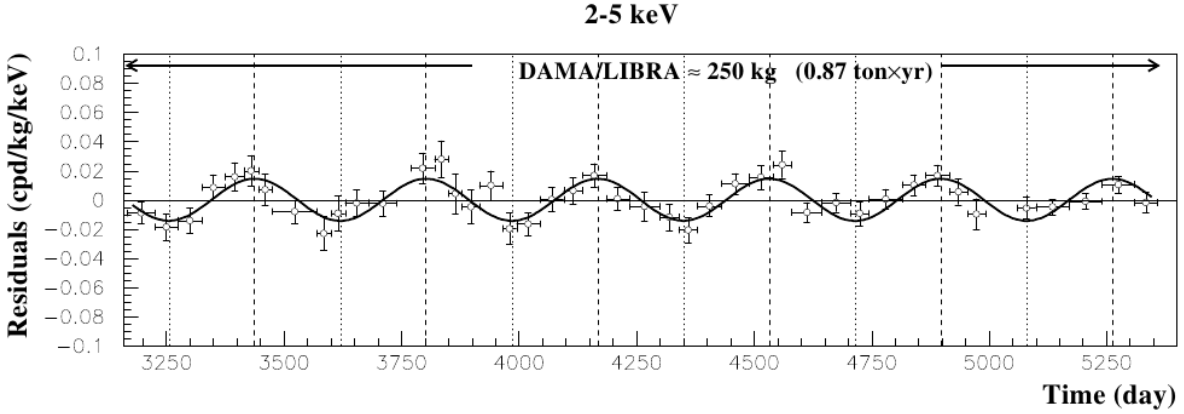

Figure 3.2: Annual modulation of a signal measured by DAMA experiment in the 2-5 keV energy interval. Number of recorded events compared to the mean number of events in a long time period (residuals) is shown[21].

Depending on the type of detector, energy of nuclear recoils can be transferred to scintillation, ionization, phonon signals or a combination thereof. The majority of experiments (such as CDMS[15], CRESST[16], EDELWEISS[17]) use cryogenic detectors operated at very low temperatures, which detect heat produced in electron and nuclear recoils. Another common technique is the use of noble liquid detectors. Here, it is possible to detect scintillation light and ionization electrons produced by a particles in their collisions in liquid xenon or argon (e.g. ZEPLIN[18], XENON[19] and ArDM[20]).

Two kind of interactions can be expected from WIMP-nucleon scattering. The first is a spin independent (SI) scalar coupling, where the WIMP couples to the nucleus as a whole ($\propto A^2$, where A is an atomic mass number). The second one is a spin dependent (SD) vector coupling ($\propto J(J+1)$, where J is spin of the nucleus). The expected event rate R is proportional to the density of DM particles ρ, cross section for WIMP-nucleus elastic scattering σ and the speed of the Earth with respect to the DM halo V:

$$R \propto \rho \cdot \sigma \cdot V. \tag{3.1}$$

The speed of the Earth with respect to the halo changes throughout a year due to combination of the Earth's motion around the Sun and the Sun motion around the Galactic Center. Therefore, with a high statistics of collected DM particle interactions one would expect to see annual modulation of an observed event rate. Such an effect was observed by DAMA[21] experiment (Fig. 3.2), which has been in operation since 1996. Experiment is based on detection of scintillation light using 250 kg of high purity NaI crystals. The periodical character of the recorded

number of counts observed by DAMA matches criteria expected for a WIMP induced signal like amplitude and phase corresponding to June/December. The experiment claims that this effect is due to observed WIMPs scatterings in the detector. Critics argue that DAMA experiment has not sufficiently proven that observed low energy signal in not due to seasonal variation of background in and around the detector. Furthermore, there are claims about dark matter signals by experiments such as CoGeNT[22], CRESST[16] and recently CDMS[15]. These seem to be consistent with a low-mass dark matter particle, possibly a mass of about 10 GeV. However, other experiments like XENON[19] and EDELWEISS[17] do not confirm this observations. The current results from direct detection experiments are shown in Fig. 3.3, where exclusion limits, allowed regions in WIMP mass and SI cross-section plane are presented. The current situation is controversial and requires confirmation in independent direct or indirect detection experiments.

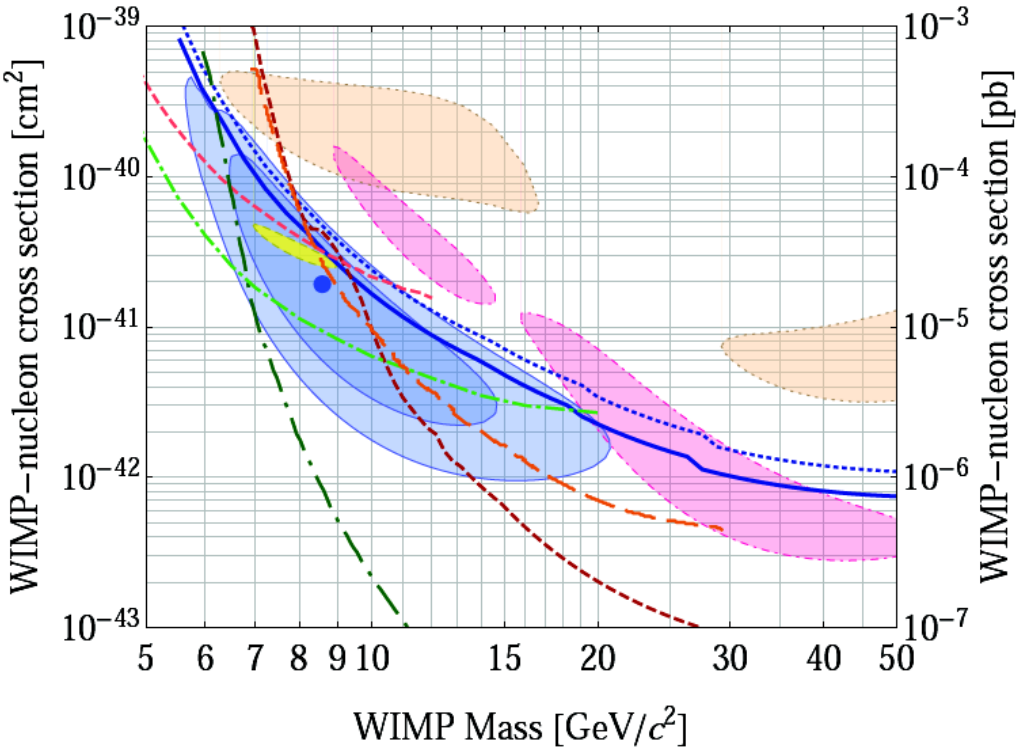

Figure 3.3: Experimental upper limits (90% Confidence Level) for the WIMP-nucleon SI cross section as a function of WIMP mass. Limit obtained from the CDMS II experiment with the exposure of 140.2 kg-days (blue dotted line), and combined limit from the CDMS II Si data set (blue solid line), limits from the CDMS II Ge standard and low-threshold analysis (dark and light dashed red), EDELWEISS low-threshold (longdashed orange), XENON10 S2-only (dash-dotted green), and XENON100 (long-dash-dotted green) are shown. The filled regions identify possible signal regions from CoGeNT (dashed yellow, 90%CL), DAMA/LIBRA (dotted tan, 99.7% CL), and CRESST (dashdotted pink, 95.45%CL) experiments. 68% and 90% CL contours for a possible signal from CDMS II experiment with the silicon detectors are shown in light blue. The blue dot shows the maximum likelihood point at (8.6 GeV/c^2, $1.9 \cdot 10^{-41}$cm^2)[15].

3.2 Indirect detection

Indirect detection experiments search for WIMP annihilation or decay products in the Universe by investigating cosmic rays. The annihilation rate is proportional to the velocity-averaged self-annihilation cross-section and numerical density squared:

$$\Gamma_A \propto < \sigma_a V > \times n_\chi^2 = < \sigma_a V > \times \frac{\rho_\chi^2}{m_\chi^2}, \tag{3.2}$$

where ρ_χ corresponds to dark matter particles density in the local halo. Most of the SUSY models assume that dark matter particles would be their own antiparticles. The pairs of WIMPs could annihilate, and depending on their mass, produce leptons, quarks, gauge or Higgs bosons (see Fig. 3.4). After subsequent decays of the primal annihilation products, various Standard Model particles can be created. The searches focus on channels and energy ranges where it is possible to reasonably disentangle dark matter induced signals from the ordinary astrophysical background. There are few viable possibilities such as gamma rays, neutrinos and antimatter. Additionally, if the WIMPs are unstable, they could also decay into Standard Model particles. In this case, the decay rate would be proportional to dark matter density.

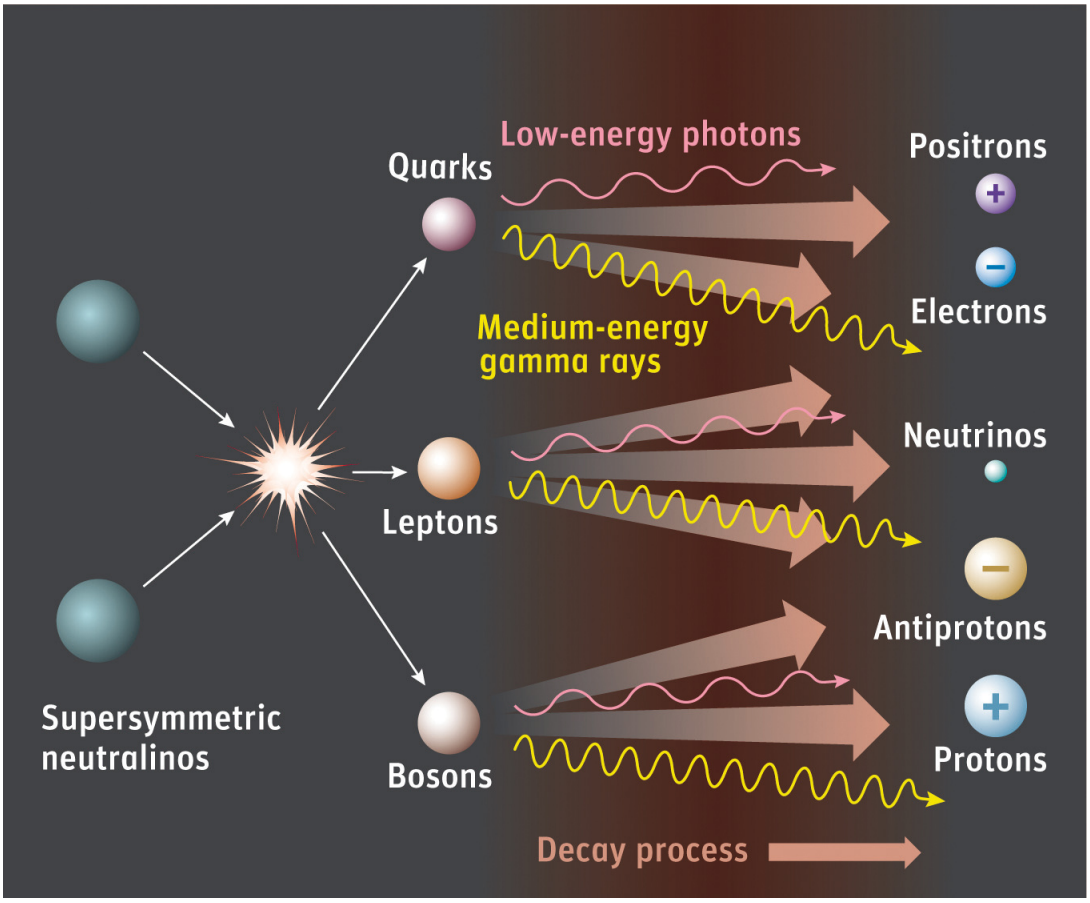

Figure 3.4: A sketch of possible products of supersymmetric dark matter self-annihilation.

3.2.1 Antimatter

Since the antimatter is much less abundant in the Universe than the ordinary matter, its excess in the cosmic rays may suggest that it originated in dark mater annihilation or decay. The searches are conducted using detectors placed on the Earth's orbit on satellites (FERMI-LAT[23], PAMELA[24] and AMS-02[25]), or on balloons (ATIC[26] and HEAT[27]). High altitudes are required to reduce background induced by primary cosmic ray interactions in the atmosphere. Data from the PAMELA satellite showed an excess of positrons from 10 GeV up to 100 GeV as compared to standard prediction of positron production in cosmic rays fluxes. The result was compatible with previous results from HEAT and AMS-01 experiments. These findings have been recently confirmed in independent measurements by FERMI and AMS-02 experiments. The most recent results from AMS-02 experiment which measured positron fraction at energies between 0.5-350 GeV showed excess above 10 GeV in the spectrum (see Fig. 3.5).

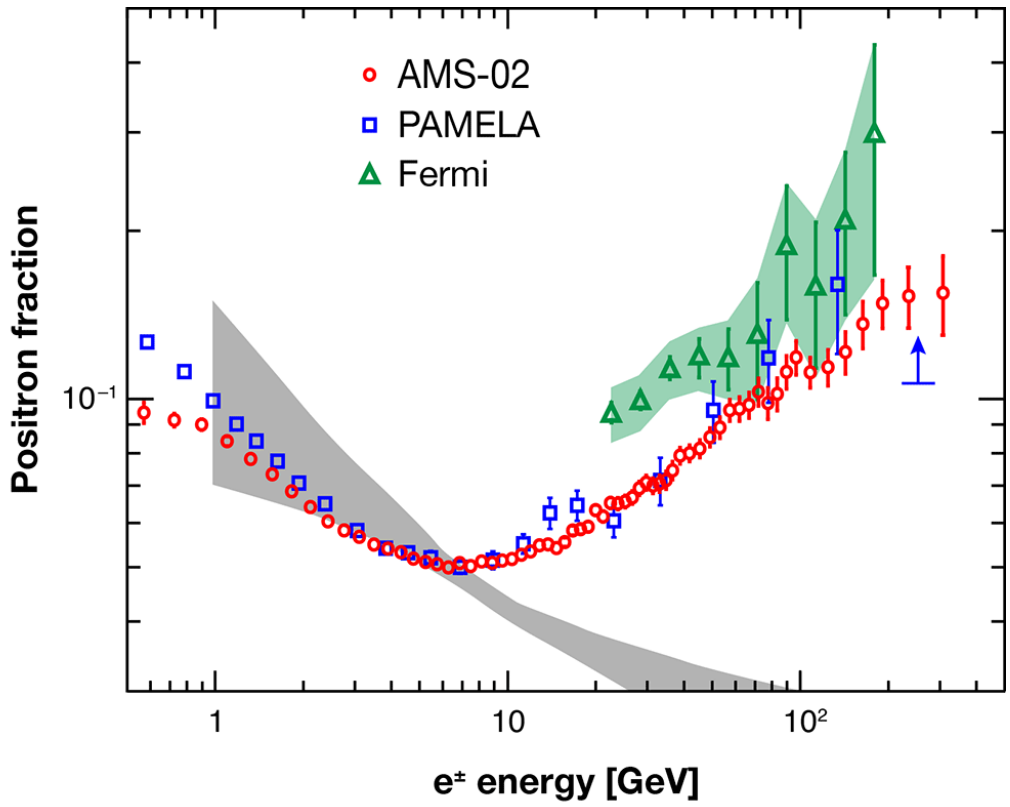

Figure 3.5: The positron fraction measured by AMS-02[25] experiment compared with the measurements from PAMELA[24] and Fermi-LAT[23]. The grey band indicates the expected range in the positron fraction due to standard production in cosmic rays.

At the same time no excess in the antiproton flux has been observed. This may indicate kind of "leptophily" of WIMPs i.e. they may annihilate almost exclusively into leptonic channels. There is a possibility that all of these experiments have seen the "smoking gun" signal of dark matter annihilation in the galactic halo, but the situation still requires confirmation in other searches.

3.2.2 Photons

Since some hints of dark matter annihilations in the positron spectrum have been observed, it is very important to consider the associated signals in the photon fluxes. Photons can be produced in many WIMP annihilation or decay channels. Their observed excess could be also a signature of DM particle annihilation/decay. Moreover, photons propagate in space without significant deflection, so they can provide good angular information of the source position, and their observed energy spectra also could be a good estimate of primary WIMP annihilation/decay spectra.

FERMI-LAT[23] experiment attempts to search for gamma-ray lines from the sky, looking at satellite galaxies, at the isotropic diffuse background, at clusters of galaxies, at diffuse gamma rays from wide regions of the galactic halo. In addition to satellite born experiments, such as FERMI-LAT, the gamma rays can be measured in Cherenkov telescopes such as MAGIC[28], HESS[29] or VERITAS[30]. HESS has also performed a large number of studies which are relevant for dark matter searches. Observations towards the Galactic Center, the Galactic Ridge, the Galactic Center Halo, a couple of globular clusters, a number of dwarf galaxies such as Sagittarius, Carina and Sculptor and Canis Major and the Fornax galaxy cluster are conducted. HESS has also looked at possible signals from spikes of DM accumulated around Intermediate Mass Black Holes. The VERITAS telescope has investigated a few dwarf spheroidal galaxies and the Coma galaxy cluster. The MAGIC telescope has investigated a few dwarf galaxies and the Perseus galaxy cluster. The overall common conclusion of almost all the studies cited above is no "anomalous" signals are individuated. Therefore, upper bounds on DM annihilation cross section can be derived in those searches.

3.2.3 Neutrinos

Some fraction of WIMPs passing through the Galactic Center, the Sun or the Earth may scatter off atoms and loose energy. Due to this process a large population of WIMPs may accumulate at the center of these celestial bodies, increasing the chance that two of them will collide and annihilate. Neutrinos could be one of the products of such an annihilation being produced directly or in subsequent decays of mesons and leptons. Neutrinos provide very good information of source position and they can be a good insight into areas where the dark matter induced signal to astrophysical background ratio can be maximized. Neutrino telescopes such as IceCube[31], ANTARES[32] and Super-Kamiokande[33] are searching for signals originating from the center of the Milky Way, the Sun or the Earth. The energy of dark matter induced neutrinos remain completely unchanged during their propagation through the cosmic space. Therefore, neutrinos can provide valuable information about energy spectra generated in dark matter annihilation. However, detection of neutrinos is very challenging due to their weak-scale cross section and the fact that they are neutral and one rely on observation of products of their interactions. This thesis presents the search for dark matter induced neutrinos from the Galactic Center using the Super-Kamiokande detector.

Chapter 4

Super-Kamiokande Detector

4.1 Introduction

Super-Kamiokande is a large water Cherenkov detector located at the Kamioka Observatory of the Institute for Cosmic Ray Research, University of Tokyo. It is operated by an international collaboration of 30 institutes from Japan, United States, Korea, China, Canada, Poland and Spain. The observatory was designed to search for a proton decay, study solar, atmospheric and man-made neutrinos, and keep watch for supernovae.

Super-Kamiokande is a successor to the Kamioka Nucleon Decay Experiment (KamiokaNDE) and Kamiokande-II experiment, which observed solar and atmospheric neutrinos, detected neutrinos from Supernova 1987A and set, what was then the world's best, limit on the lifetime of the proton. The construction of the Super-Kamiokande started in 1991 and the observation began in 1996. The detector contained fifteen times more water and ten times more photomultipliers (PMTs) than Kamiokande[34]. In 1998 the Super-Kamiokande Collaboration announced the evidence of atmospheric neutrino oscillation, which was the first experimental observation supporting the theory that the neutrino has a non-zero mass[35]. In 2001, solar neutrino oscillations were confirmed[36]. Precise measurement of the solar neutrino flux allowed for investigation of the activities inside of the Sun. Moreover, more stringent limits on a proton decay were set.

On November 2001, about half of the photomultiplier tubes imploded during the water refilling process. After this accident the detector was partially restored by redistributing the remaining PMTs, and operated as SK-II phase. In July 2005, the detector reconstruction began to its original form by installation of remaining PMTs. The work was completed in June 2006. This phase of the experiment is being reffered as SK-III and spans data collection period from October 2006 till August 2008. The current experimental phase started in September 2008 after significant upgrades to the experiment's electronics and it is referred to as SK-IV phase. Experiment continues to run, collecting data on various natural sources of neutrinos, as well as acting as the far detector for the Tokai-to-Kamioka (T2K) long baseline neutrino oscillation experiment[37].

4.2 Detector Construction

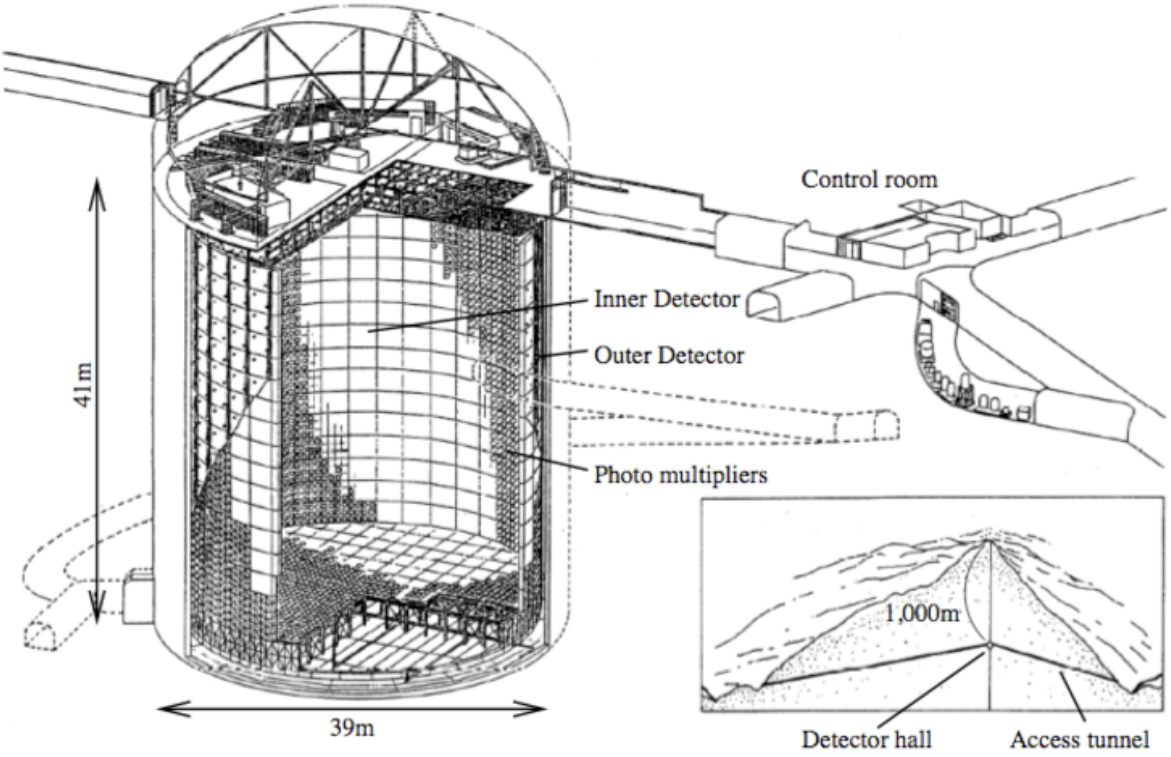

Figure 4.1: A drawing of the Super-Kamiokande detector and the experimental hall[37].

The Super-Kamiokande detector is located 1,000 m underground in the Mozumi Mine of the Kamioka Mining and Smelting Co. near the Kamioka section of the city of Hida in Gifu Prefecture. The mountain above the detector reduces the rate of cosmic ray muons by a factor of 1/100,000 with respect to the ground surface. Super-Kamiokande detector is a cylindrical stainless steel tank, 42m tall and 39m in diameter, holding 50,000 tons of ultra-pure water being monitored by PMTs. In addition, detector consists also of water and air purification system, electronics, online data acquisition system, and offline computer facilities. The schematic view of the detector and experimental hall is presented in Fig. 4.1. The tank volume is divided into an inner detector (ID) region that is 34m in diameter and 36m in height, and outer detector (OD) which consists of the remaining tank volume. The inner part and outer part are optically isolated using high reflectivity tyvek sheets. Inner detector contains 11,146 20-inch PMTs mounted on the tank wall. In the outer detector 1,885 8-inch PMTs are installed facing outside. This solution allows to identify muons coming from outside the tank and also to make the inner part free from gamma rays and neutrons from the rock.

4.3 Principle of Operation

Neutrinos do not have electric charge, which means that they are not affected by the electromagnetic forces and interact only via week interactions. Therefore, neutrinos pass through normal matter unimpeded and are very difficult to detect. Occasionally neutrinos can interact

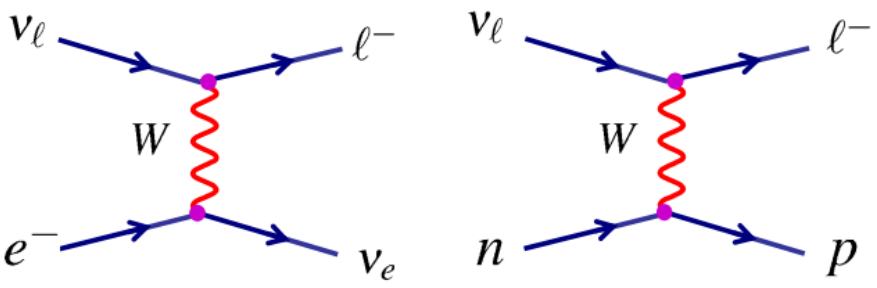

Figure 4.2: Charged current (CC) neutrino interactions (via a W-boson exchange).

with the electrons or nuclei and produce a charged particle (see Fig. 4.2). Not all interactions are kinematically allowed, i.e. there is a threshold energy for interaction to occur. Sufficient energy in the centre-of-mass frame to produce the final state particles is required.

Detection of neutrino interaction is based on observation of charged particle produced in this process. When the generated charged particle moves faster than the speed of light in water, it produces electromagnetic wave known as Cherenkov radiation. The Cherenkov light when projected onto the walls of the detector forms a characteristic shape of rings. This light is recorded by the PMTs. The energy, direction and neutrino interaction point can be reconstructed based on the amount of charge deposited in PTMs and the time when the light was detected. The direction of a parent neutrino and direction of a produced charged lepton are correlated. If the neutrino is more energetic, the produced lepton closer follows the original direction of its parent neutrino.

Particle flavor is conserved in neutrino interactions. Electron neutrino interacting via charge-current boson exchange would produce electron, muon neutrino produces muons, and tau neutrino produces tau lepton. The type of the charged particle produced in neutrino interaction can be inferred from the sharpness of the edge of the ring which is presented in Fig. 4.3. The multiple scattering of electrons is large, so electromagnetic showers produce fuzzy rings. Highly relativistic muons, in contrast, travel almost straight through the detector and produce rings with sharp edges.

4.4 Atmospheric Neutrinos at Super-Kamiokande

Neutrinos are the second (after photons) most abundant particles in the Universe. They are mostly created in nuclear reactions taking place inside stars, radioactive decays, or in weak decays of mesons and muons. Neutrino energy spectra from various sources are shown in Fig. 4.4. Among all that sources it is worth to discuss atmospheric neutrinos as they would have the same energies as expected for dark matter induced neutrinos. Atmospheric neutrinos are produced in interactions of cosmic rays with atomic nuclei in the Earth's atmosphere. That leads to creation of showers of particles, many of which are unstable and produce neutrinos when they decay. The average energy of atmospheric neutrinos is of several hundreds of MeV and the energy spectra has a long high energy tail reaching TeV scale. If dark matter exist, it

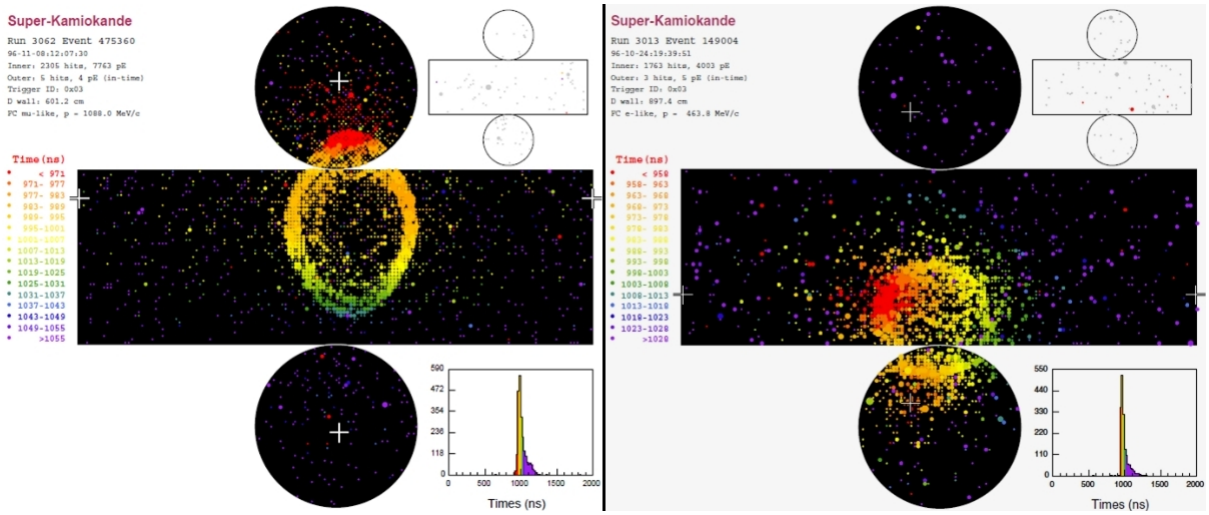

Figure 4.3: An example event display of single-ring μ-like (left) and e-like (right) event. The colored points indicate the quantity of the detected light by each PMT.

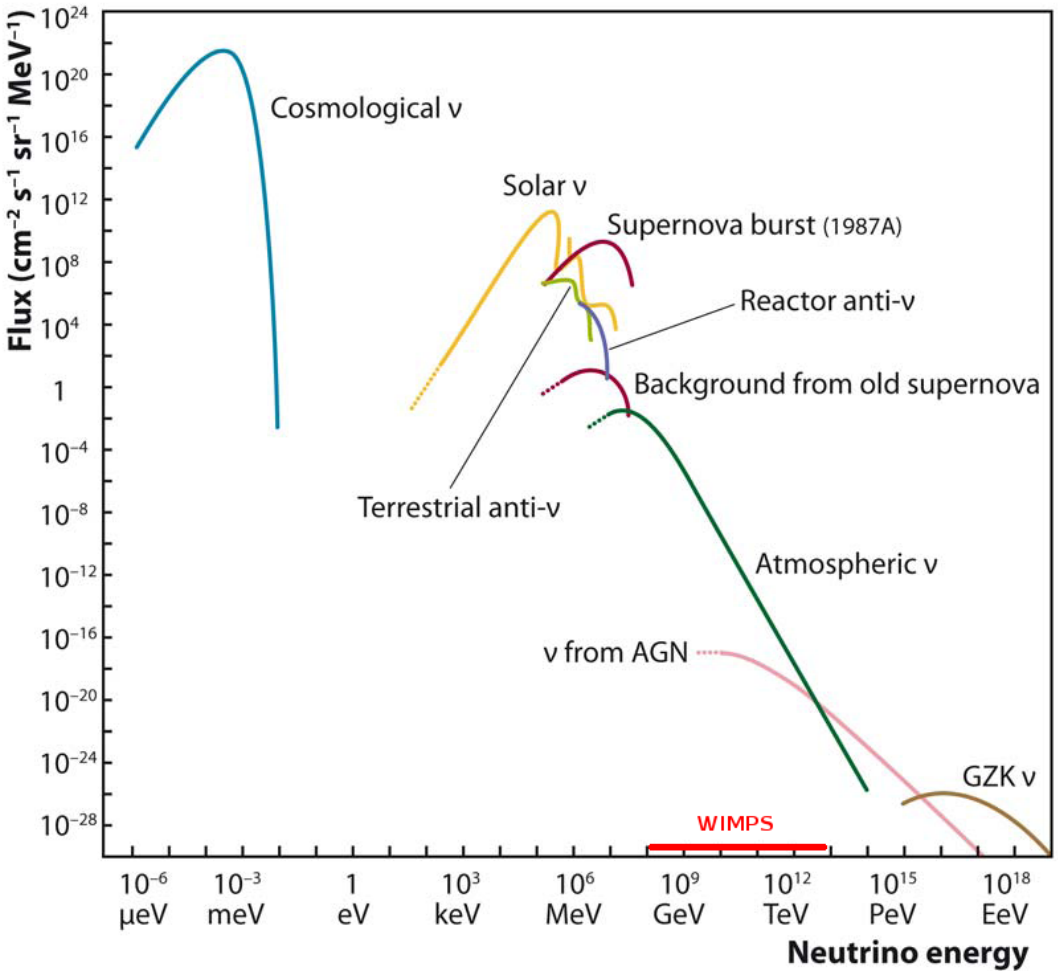

Figure 4.4: Neutrino energy spectrum for various neutrino sources.

is expected that observed atmospheric neutrinos may contain some contribution of dark matter induced neutrinos. The aim of the analysis presented in this thesis is to evaluate the allowed contribution from this hypothetical additional source.

4.4.1 Event Classification

In the Super-Kamiokande detector, the interactions of low energy (100 MeV-10 GeV) atmospheric neutrinos are observed via their charged-current interactions. If the produced charged particle stops in the inner detector, interactions are classified as fully-contained (FC). If a high energy lepton exits the inner detector and deposit energy also in the outer veto region, events are classified as partially-contained (PC). The energies of neutrinos which produce partially-contained events are typically 10 times higher that those, which produce fully-contained events. Neutrinos also interact with the rock surrounding the detector and produce high energy muons which intersect the tank. Downward-going muons produced in interactions of neutrinos cannot be distinguished from the constant flux of cosmic ray muons. However, muons travelling in upward direction must be neutrino induced. Upward-going muons (UPMU) sample can be divided into upward stopping muons, which enter the detector and stop inside, and upward through-going muons, which traverse the entire detector volume. The parent neutrinos which produce upward through-going events are significantly more energetic than stopping muon events. Additionally one can distinguish subsample of showering events among upward through-going muons, which are produced by potentially the most energetic neutrinos, with energies of about hundreds of GeV. The expected number of neutrino events in each class as a function of neutrino energy is presented in Fig. 4.5.

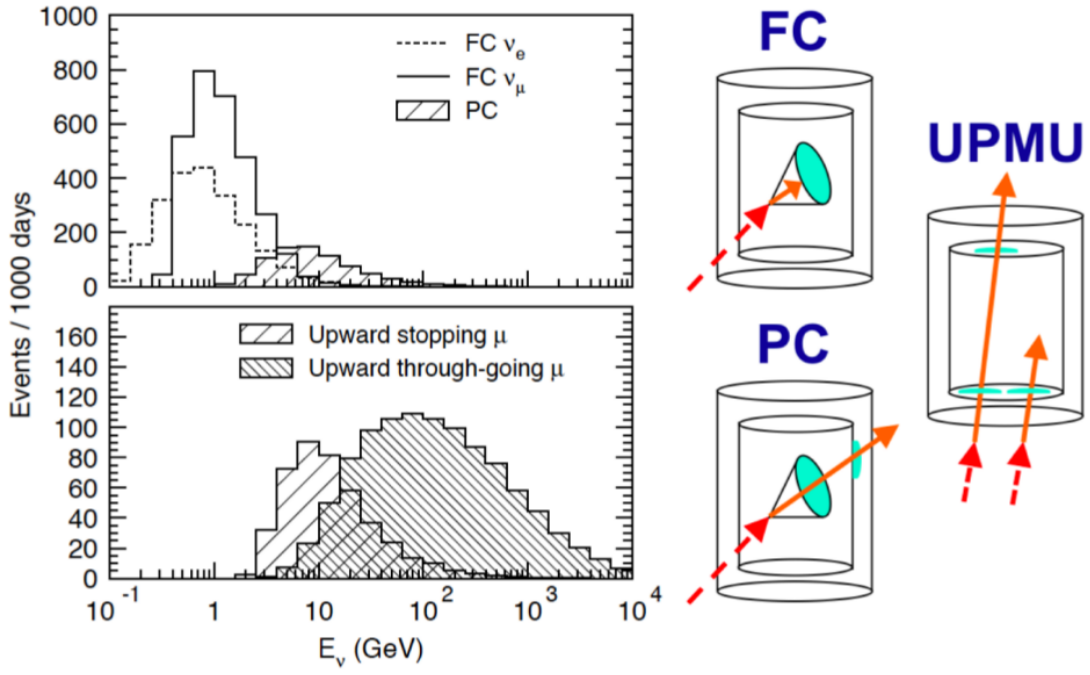

Figure 4.5: The expected parent neutrino energy distributions for the fully-contained, partially-contained, upward stopping-muon and upward through-going muons samples.

Chapter 5

Milky Way Halo Models

5.1 Dark Matter Halo

Indirect searches aim at detection of dark matter annihilation/decay products in the fluxes of cosmic rays, such as charged particles, photons or neutrinos. Since expected signals depend on the square of the dark matter density for annihilation or are proportional to density in case of decay, the distribution of dark matter in the Universe is crucial for robust predictions.

It is expected that dark matter halo envelops the galactic disk and extends far beyond the edge of the visible galaxy. In the ΛCDM model, dark matter halos are assumed to form hierarchically via gravitational amplification of initial density fluctuations (bottom-up). Cosmological N-body simulations with large dynamic range[38] and gravitational lensing observations[6] seem to indicate that dark matter density profiles can be described in the form:

$$\rho(r) = \frac{\rho_0}{(r/r_s)^{\gamma}[1+(r/r_s)^{\alpha}]^{(\beta-\gamma)/\alpha}}, \tag{5.1}$$

where the parameters α, β, γ and r_s take different numerical values for different models. Parameter γ is the inner cusp index, r_s is the scale radius and the normalization ρ_0 is chosen so that the mass contained within the solar circle ($R_{sc} = 8.5$kpc) provides the appropriate dark matter contribution to the local rotational curves. In addition, to avoid numerical divergences due to very cuspy profiles (which may be an artifact of simulations), one assumes a flat core for all the profiles in the innermost 0.1° around GC.

Table 5.1: The parameters of Eq. 5.1 for considered profiles.

Halo Model	α	β	γ	r_s [kpc]	$\rho(R_{sc})$ [GeV/cm^3]
NFW	1	3	1	20	0.3
Moore	1.5	3	1.5	28	0.27
Kravtsov	3	3	0.4	10	0.37

The three commonly used profiles are Navarro-Frenk-White[40], Moore[41] and Kravtsov[42], and parameters corresponding to this models are listed in Table 5.1. The comparison of the dark matter density distribution, $\rho(r)$, as a function of distance from the Galactic Center for considered profiles is shown in Fig. 5.1. For the outer regions of the halo (several kpc away from the

Galactic Center) one can observe very similar behaviour and good agreement between profiles. However, the inner gradient of the halo profile is the most uncertain part, due to the spatial resolution limit of the existing simulations. In the analysis presented in this thesis, the NFW profile will be used as a benchmark model, while the Moore and Kravtsov profiles will be applied as extreme cases to estimate the influence of halo model choice on the obtained results.

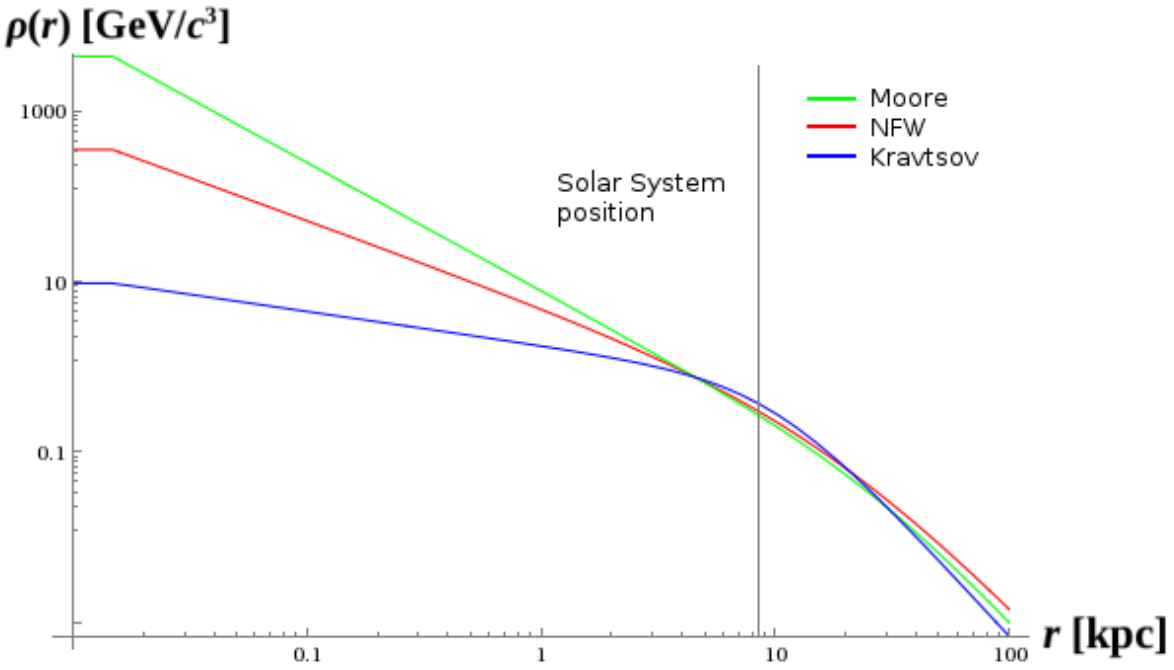

Figure 5.1: The dark matter density versus distance from the GC for three considered profiles.

5.2 Spectrum of Dark Matter Annihilation Products

The intensity J (number flux per solid angle) of dark matter annihilation products in the galactic halo at an angle Ψ with respect to the GC direction is proportional to the dark matter density squared integrated along the line of sight[14] (see Fig. 5.2 for definition of the variables):

$$J(\Psi) = \frac{1}{R_{sc}\rho_{sc}^2} \int_0^{l_{max}} \rho^2(\sqrt{R_{sc}^2 - 2lR_{sc}\cos\Psi + l^2})dl. \tag{5.2}$$

The prefactor $\frac{1}{R_{sc}\rho_{sc}^2}$, where $\rho_{sc} = \rho(R_{sc})$ is an arbitrary scaling which makes $J(\Psi)$ dimensionless. The upper limit for integration l_{max} is defined as:

$$l_{max} = \sqrt{R_{MW}^2 - R_{sc}^2 \sin^2\Psi}, \tag{5.3}$$

where $R_{MW} = 40$kpc is the adopted Milky Way halo size. Any enhancement of the density would result in a sharp increase in the flux of annihilation products. Since dark matter radial

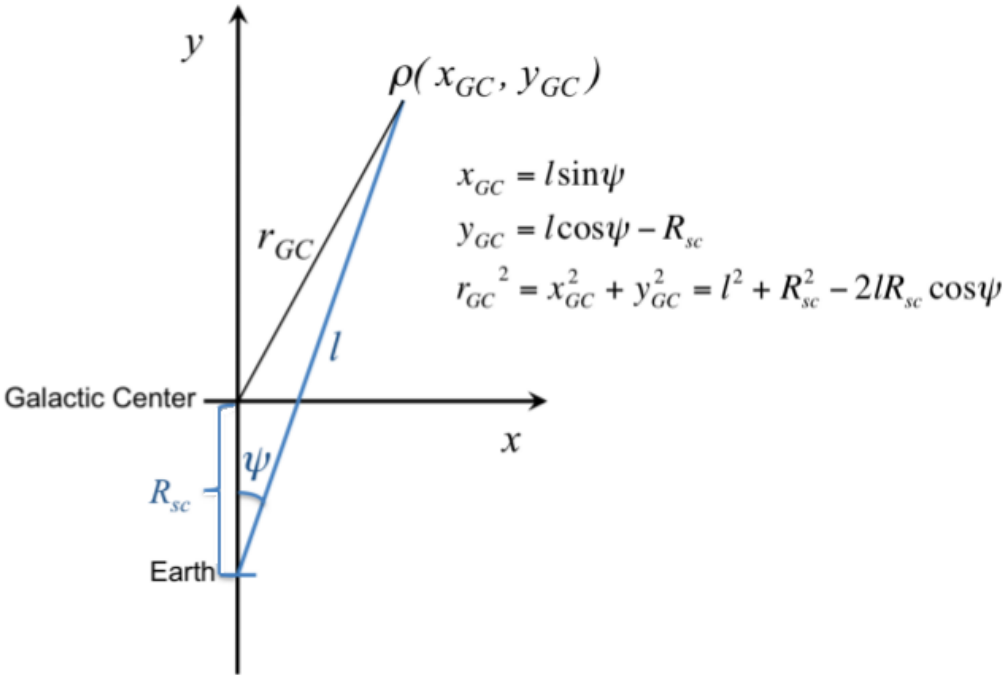

Figure 5.2: Illustration of the line of sight l and the angle Ψ in the coordinate system related to the Galactic Center.

halo profiles are peaked towards the Galactic Center one can expect very large enhancements for small angles Ψ around this point. This is presented in Fig. 5.3 for the NFW, Moore and Kravtsov profiles. One can see that intensity strongly depends on the chosen profile and the differences can be orders of magnitude at small angles. Presented density and intensity profiles had been calculated based on Eq. 5.1 and 5.2 using computational software program Mathematica [43]. The relevant quantity in a measurement is related to overall intensity of DM annihilation products received from a given cone half-angle. The integral of $J(\Psi)$ over the solid angle $\Delta\Omega = 2\pi(1-\cos\Psi)$ can be defined as:

$$J_{\Delta\Omega} = \frac{1}{\Delta\Omega}\int_{\Delta\Omega} J(\Psi)d\Omega, \tag{5.4}$$

where $\Delta\Omega$ is chosen search region. Then, the differential flux of annihilation products from this field of view can be expressed in the form:

$$\frac{d\Phi_{\Delta\Omega}}{dE} = \frac{<\sigma_A v>}{2} J_{\Delta\Omega}\frac{R_{sc}\rho_{sc}^2}{4\pi m_\chi^2}\frac{dN}{dE}. \tag{5.5}$$

The factor 1/2 accounts for DM being its own antiparticle, $1/4\pi$ is for isotropic emission of the annihilation products, m_χ is assumed mass of the DM particle and dN/dE is the spectrum of the annihilation products.

In the analysis presented in this thesis we focus on annihilation into pairs of neutrinos, $\chi + \chi \rightarrow \bar{\nu} + \nu$. In this case, the spectrum of the neutrinos per flavour is a monochromatic line with

$dN/dE = \frac{2}{3}\delta(E - m_\chi)$, where the prefactor 2/3 arises under the assumption that 2 neutrinos are produced per one annihilation of DM particles pair and all neutrino flavours are equally populated. Such mono-energetic neutrinos are of a specific interest as they can be used to set a model independent limit on the total dark matter self-annihilation cross-section into Standard Model final states[14].

For calculation of the dark matter induced neutrino flux at the Earth a full mixing is assumed due to long-baseline oscillations. The expected number of ν events observed in the detector can be found by integrating the differential neutrino flux $\frac{d\Phi_{\Delta\Omega}}{dE}$ over the detector live-time and the direction- and energy-dependent effective area for annihilation. Therefore, using Eq. 5.5 one can relate the velocity-averaged self-annihilation cross-section $< \sigma_A v >$ with dark matter induced flux and convert it into expected number of neutrinos.

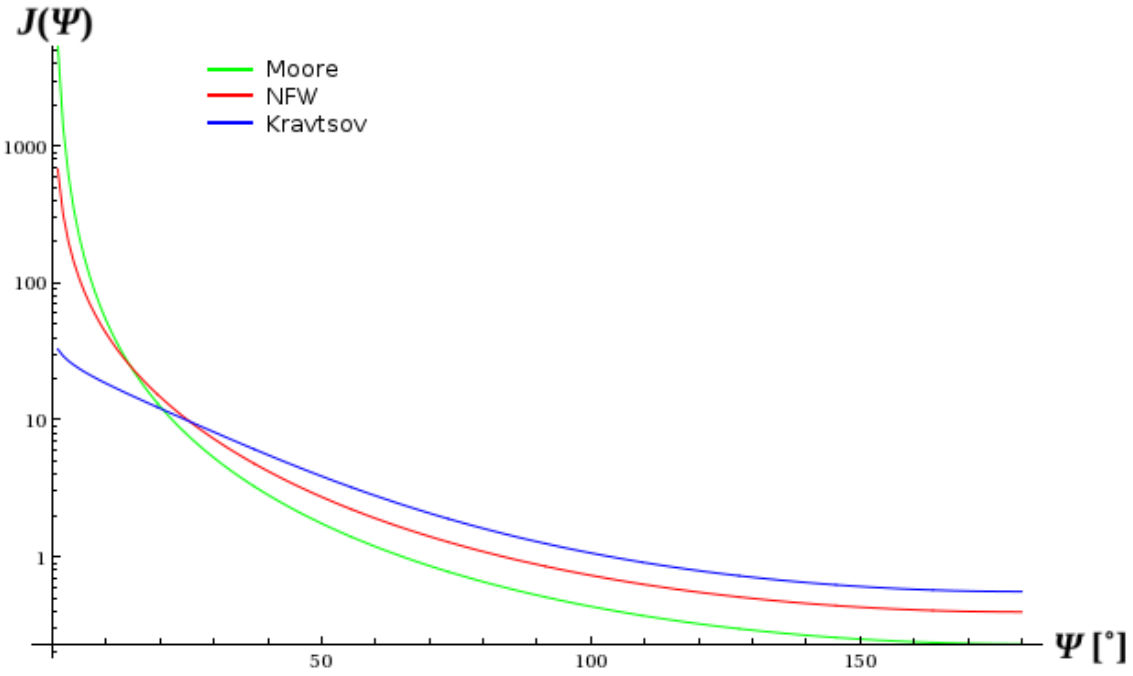

Figure 5.3: Intensity of DM annihilation products versus angular distance from the GC for three considered profiles.

Chapter 6

Search for Dark Matter from the Galactic Center

6.1 Analysed Data

The analysis presented in this thesis is based on atmospheric neutrino data collected with Super-Kamiokande detector in years 1996-2008 (SK-I, SK-II and SK-III data taking periods, see Sec. 4.1). The livetime of each sample, which corresponds to the period of time when detector was performing well, is listed in Table 6.2. The upward-going muon data set relies mostly on fitting long muon tracks, therefore depends less on detector effects, resulting in looser data quality cuts and higher livetime comparing to FC/PC sets.

Table 6.1: Livetime of SK-I, SK-II and SK-III data sets.

Sample	SK-I	SK-II	SK-III
FC/PC	1489.2 days	798.6 days	518.1 days
UPMU	1646.0 days	828.0 days	635.6 days

6.2 Monte Carlo

Neutrino interactions at Super-Kamiokande are simulated with large statistics corresponding to 500 years of livetime for each running period (SK-I, SK-II and SK-III)[44]. These generated samples are being referred to as atmospheric Monte Carlo (MC) samples and they are used also in the analysis presented here. Simulated sets contain interactions of atmospheric neutrinos with the nuclei of water, or in the case of upward muons, the nuclei of elements in the rock surrounding the detector. Charged and neutral current neutrino interactions (quasi-elastic scattering, single meson production, coherent π production and deep inelastic scattering) are considered. The detector response for neutrino interaction products is included and the same data reduction procedure is applied to MC events as to real data. Therefore after scaling to the data livetime, one can obtain expected number and characteristics of atmospheric events seen in the experiment.

6.3 Equatorial Coordinate System

In the search for dark matter induced neutrinos originating in the Galactic Center, it is very convenient to use equatorial coordinate system (see Fig. 6.1). Its origin is defined at the center of the Earth and the fundamental plane is formed by projection of the Earth's equator onto the celestial sphere, forming the celestial equator. A primary direction is pointing towards the vernal equinox, which is one of the two points where the ecliptic intersects the celestial equator. To determine the position of a point in this system, two coordinates are used. The first one is declination (DEC), which measures the angular distance of an object perpendicular to the celestial equator, positive to the north and negative to the south. Declination is analogous to terrestrial latitude. The second coordinate is right ascension (RA) which measures the angular distance of an object eastward along the celestial equator from the vernal equinox and is similar to terrestrial longitude.

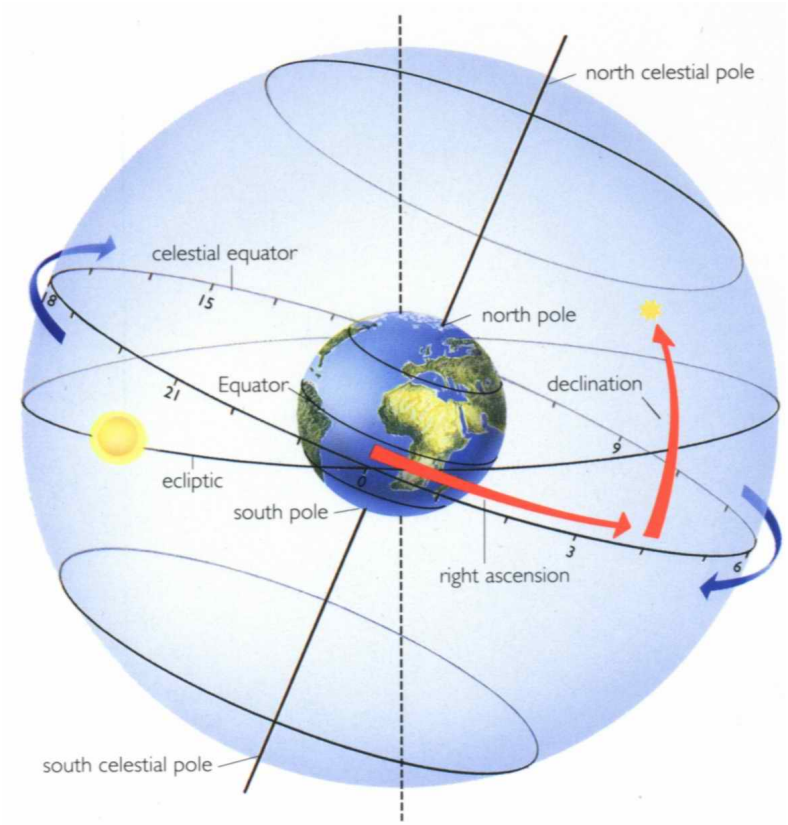

Figure 6.1: Definition of coordinates in equatorial coordinate system[45].

One of the advantages of the equatorial coordinate system is the fact that it does not rotate with the Earth, but remains fixed against the background stars. This is very convenient as then the star's positions do not depend on the position of the observer and also the position of the Galactic Center is fixed, which is crucial for this analysis (see Fig. 6.2). On the contrary, in the horizontal coordinate system, a star's position differs among observers based on their positions on the Earth's surface, and is continuously changing with the Earth's rotation.

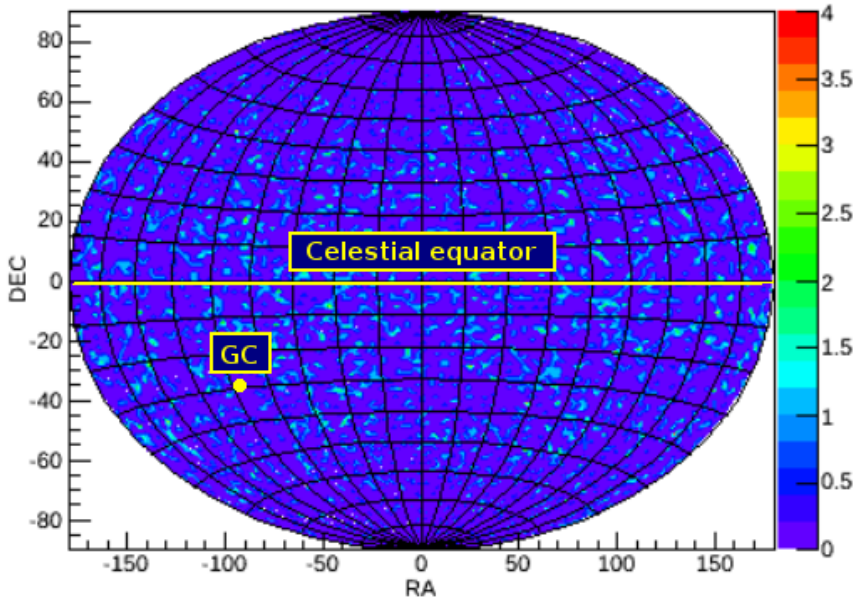

Figure 6.2: Atmospheric neutrino events from SK-I data set in equatorial coordinate system.

6.4 Simulation of WIMP Induced Neutrinos

The Galactic Center region is expected to contain the largest density of dark matter. In the considered halo models, neutrinos originating from dark matter annihilation would introduce a significant modification to distribution of atmospheric neutrino events observed in equatorial coordinate system, where the position of the Galactic Center is fixed. Since the calculation of the spectrum of annihilation products is well established (see Chapter 5.), one can try to simulate the neutrino events originating in this process in order to investigate expected signal properties.

The following analysis is focused on the study of neutrino's directions and their distribution around the GC. The Monte Carlo simulation of interactions of atmospheric neutrinos, which is available for the Super-Kamiokande data in large statistics, is used to simulate the expected WIMP-induced neutrino events (signal). Atmospheric neutrinos (background) are isotropic in equatorial coordinate system, but DM-induced neutrinos are expected to be peaked from the direction of the GC (as the dark matter annihilation is proportional to density squared, see Sec. 5.2). To every event in atmospheric Monte Carlo one can assign WIMP weight, in order to obtain the characteristic shape associated with dark matter density distribution. At a certain angular distance $\Psi > 1^\circ$ from the Galactic Center, WIMP weight is equal to intensity:

$$\text{WIMP weight}(\Psi) = J(\Psi), \tag{6.1}$$

for 1° intervals.

The intensity profile has a very sharp shape for small angular distances from the Galactic Center. To take into account this effect, the finer weights binning were applied below $\Psi < 1^\circ$. In this analysis, the three sets of WIMP weights were used in order to reproduce signal shape for three considered dark matter halo models (NFW, Moore and Kravtsov).

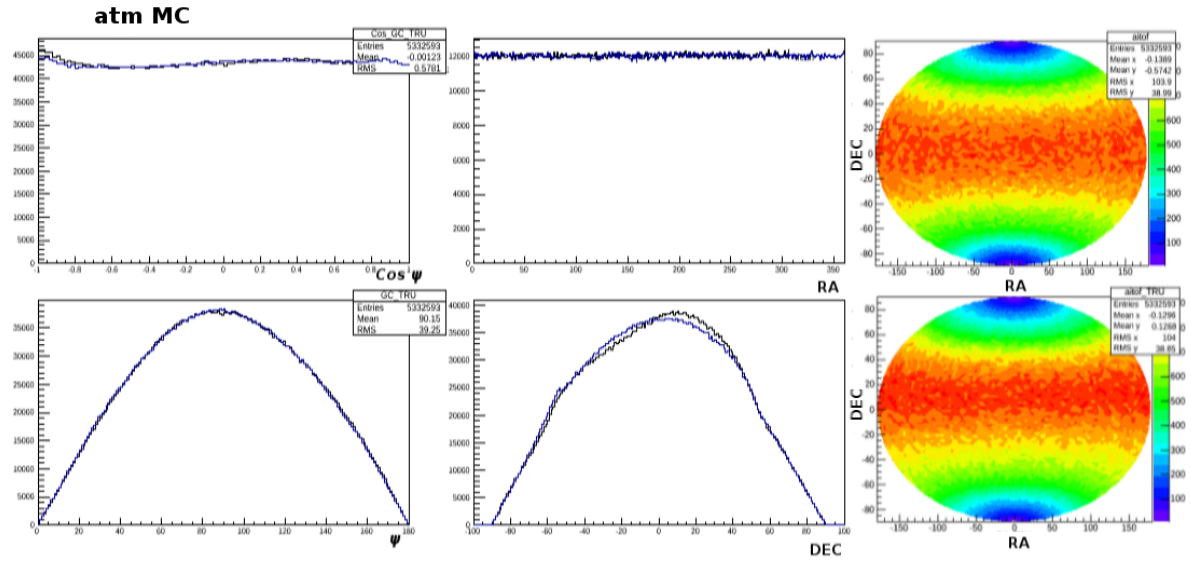

Figure 6.3: Distribution of the cosine of the angular distance from GC (upper left plot), the angular distance from GC (bottom left plot), right ascension (upper middle plot), declination (bottom middle plot), and spherical projections in equatorial coordinate system (upper right plot for reconstructed and bottom for true directions) of ν_μ and $\bar{\nu}_\mu$ atmospheric Monte Carlo events (1500 years of livetime). Black curves correspond to true neutrino directions and blue curves to the reconstructed directions of leptons produced in ν interactions.

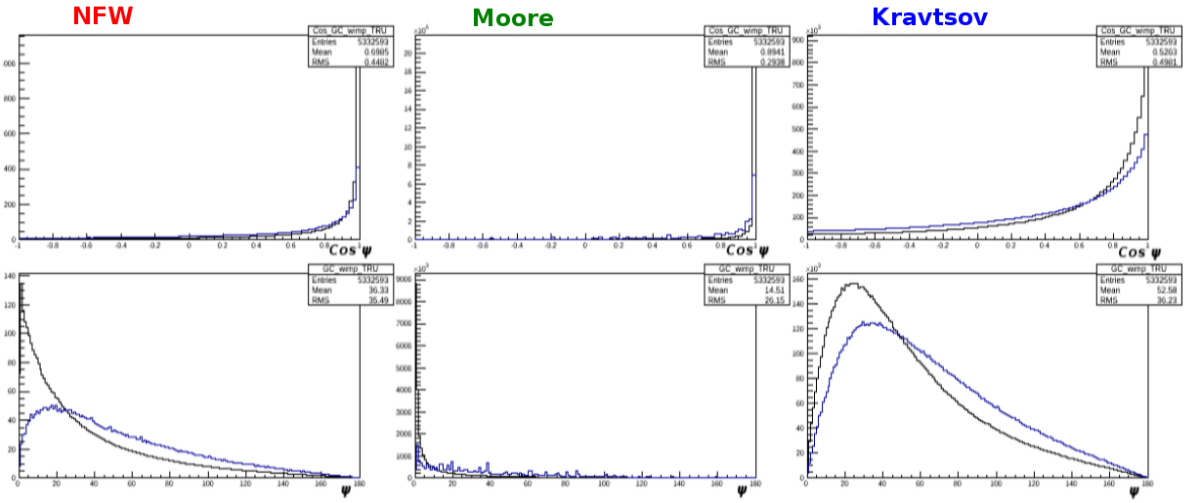

Figure 6.4: Expected signal shape in the cosine of the angular distance from GC (upper plots) and the angular distance from GC (bottom plots). Plots obtained using atmospheric muon Monte Carlo with WIMP Weights for NFW, Moore and Kravtsov profiles. Black curves correspond to true directions and blue curves to the reconstructed ones.

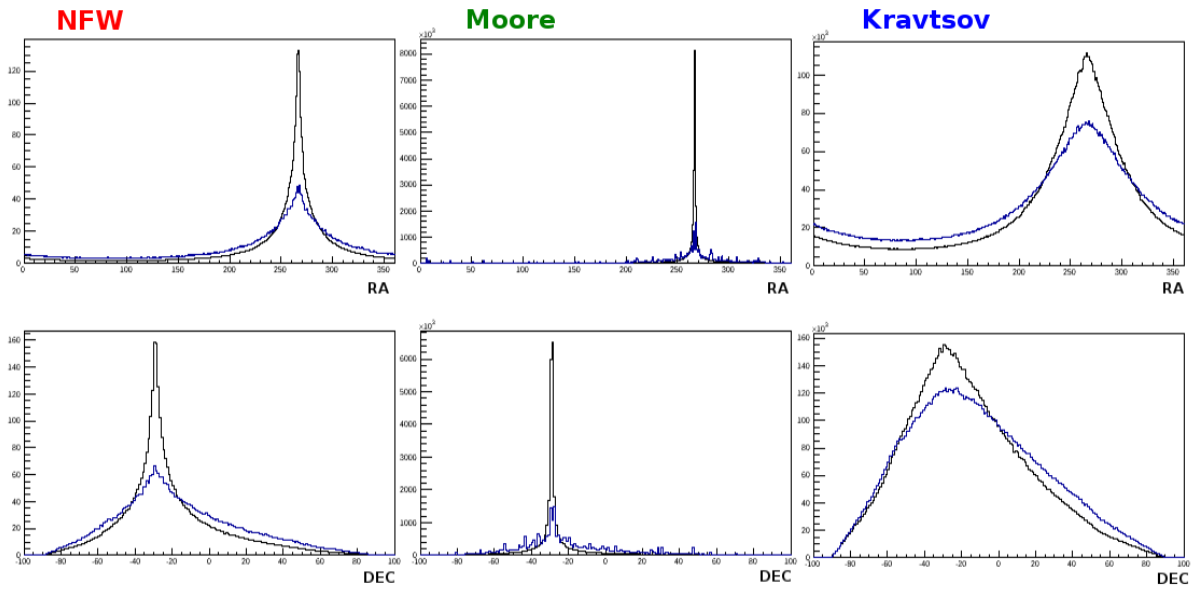

Figure 6.5: The same as in Fig. 6.4, but for right ascension (upper plots) and declination (bottom plots).

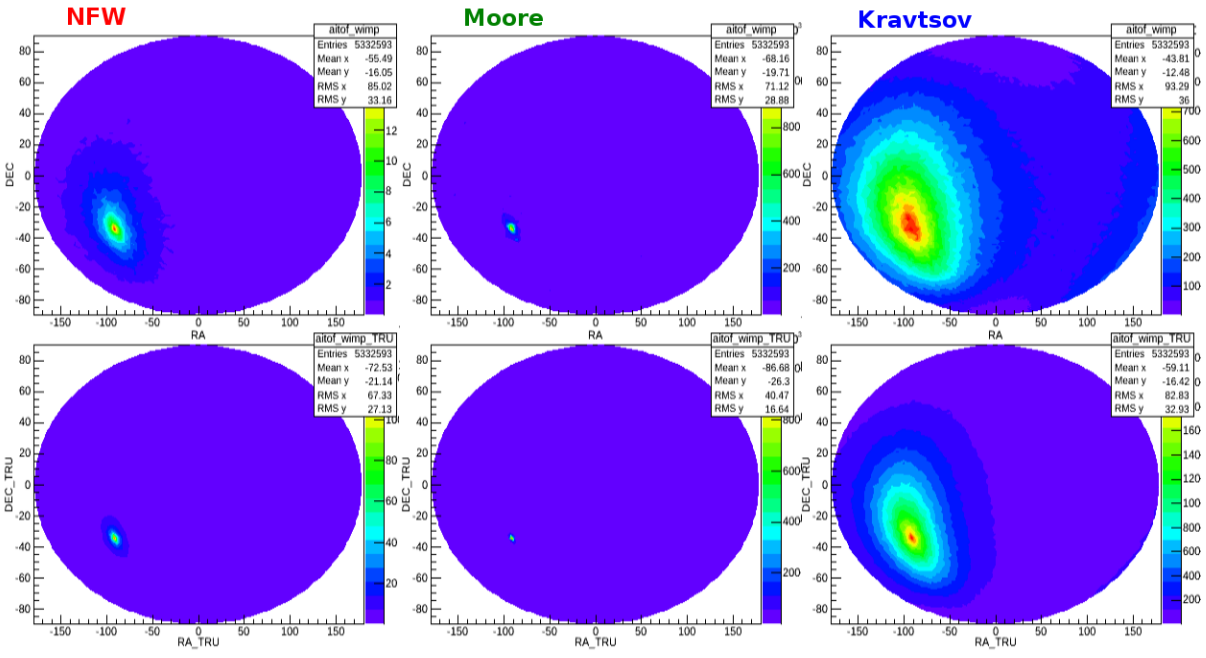

Figure 6.6: Spherical projections of the expected signal shape in equatorial coordinate system for NFW, Moore and Kravtsov profiles (upper plots for reconstructed lepton direction and bottom for true ν directions).

In Fig. 6.3 various distributions of atmospheric ν_μ MC events are shown: cosine and angle with respect to the Galactic Center, right ascension, declination, and spherical projections in equatorial coordinate system. For each plot, the true neutrino direction and reconstructed direction (based on direction of lepton produced in neutrino interaction) are shown. Based on these events and calculated WIMP weights one can obtain expected signal shape for three considered halo profiles (Fig. 6.4-6.6). The differences between three considered profiles and the effect of reconstruction procedure are clearly visible.

The results of the simulation are consistent with expectations. For each halo model, the signal is peaked and pointing towards to the Galactic Center direction. The angular resolution of the detector makes the observed signal more smooth and shows necessity to take into account precision in direction reconstruction in the analysis. The difference between profiles can be clearly seen. One can expect differences in obtained results due to adopted halo model.

6.5 Analysis Idea

Dark matter induced neutrino flux would manifest itself through a large scale anisotropy with the largest excess of neutrino flux at the area of the Galactic Center, as it is shown in previous section. To test this hypothesis, two regions on the sky are defined. The on-source region is centered on the Galactic Center position (266° RA, -29° DEC) and defined by a circle around this point with a half-opening angle Ψ. The off-source region is equally-sized, but offset by 180° in RA (see Fig. 6.7).

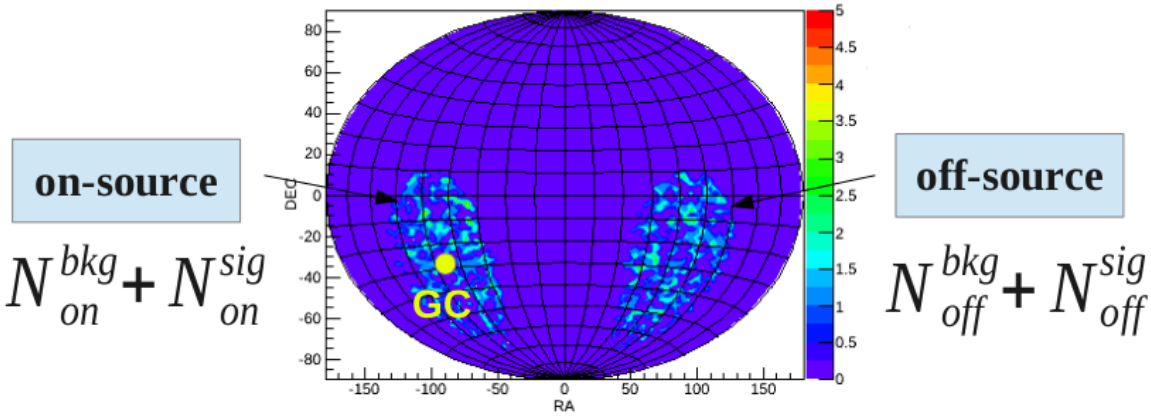

Figure 6.7: Analysis idea.

In both regions signal and background events are expected. Signal events are defined as dark matter induced neutrinos. Background events consist of atmospheric neutrinos which are expected to be equally distributed in the on- and off-source regions. Therefore, the difference in number of neutrino events between on- and off-source regions should contain no background events. In this way the background can be estimated directly from the data. This method is independent on atmospheric ν Monte Carlo simulations and related systematic uncertainties as

they should equally affect on- and off-source regions. The difference in number of neutrino events between on- and off-source regions correspond to difference in signal events:

$$\Delta N = (N_{on}^{bkg} + N_{on}^{sig}) - (N_{off}^{bkg} + N_{off}^{sig}) \approx N_{on}^{sig} - N_{off}^{sig} = \Delta N^{sig}. \quad (6.2)$$

The difference in signal events is directly proportional to the dark matter self-annihilation cross-section $< \sigma_A v >$. Presented analysis concept is similar to analysis performed in the IceCube experiment[31].

6.6 Optimization of the signal region size

The angular resolution of the detector strongly depends on the energy of parent neutrinos. Leptons produced in interactions of low energy neutrinos ($\leq$1 GeV) loosely follow the direction of the parent neutrino (see Sec. 4.3). The average angular separation between true parent neutrino direction and reconstructed lepton direction is shown in Fig. 6.8 for various event classes used in the analysis (FC, PC, UPMU). In addition, based on visible energy of event, FC sample can be divided into two subsamples, SubGeV ($E_{vis} < 1.33$ GeV) and Multi GeV ($E_{vis} \geq 1.33$ GeV).

At this point it is possible to optimize the analysis. The goal is to choose the optimal size of the on-source region so that signal to background ratio is maximal. Signal corresponds to DM-induced neutrinos, and background consists of atmospheric neutrinos. The optimization is performed for NFW profile, which is a benchmark model in this analysis. The angular resolution of the detector differs between classes and it is advantageous to carry out the optimization separately for SubGeV and MultiGeV fully-contained, partially contained and upward-going muon events. The results of optimization for different event classes are listed in Tab. 6.2 and shown in Fig. 6.9. The optimization of the size of the on-source region was performed entirely with simulated events. However, this is the only part of analysis where Monte Carlo events are used, later, the analysis is based only on data in order to avoid dependence of simulations and related systematic uncertainties.

Table 6.2: Results of the optimization of an on-source region.

Event class	Optimal size [°]
FC SubGeV	80
FC MultiGeV	30
PC	20
UPMU	10
ALL	35

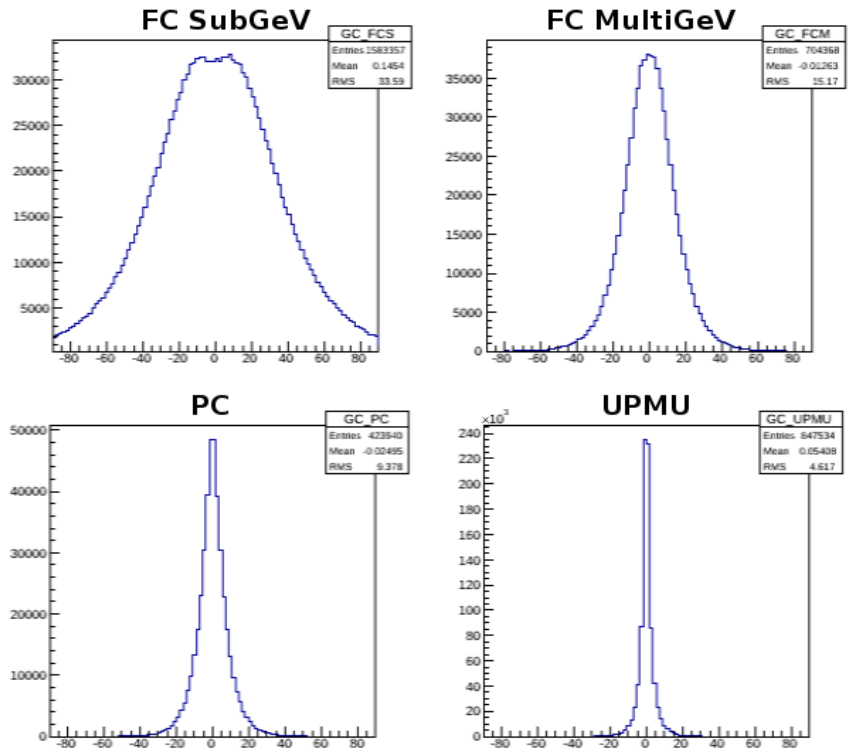

Figure 6.8: The angular difference between true neutrino direction and the reconstructed directions of leptons produced in ν interactions for different event classes, for 1500 years of atmospheric ν Monte Carlo events.

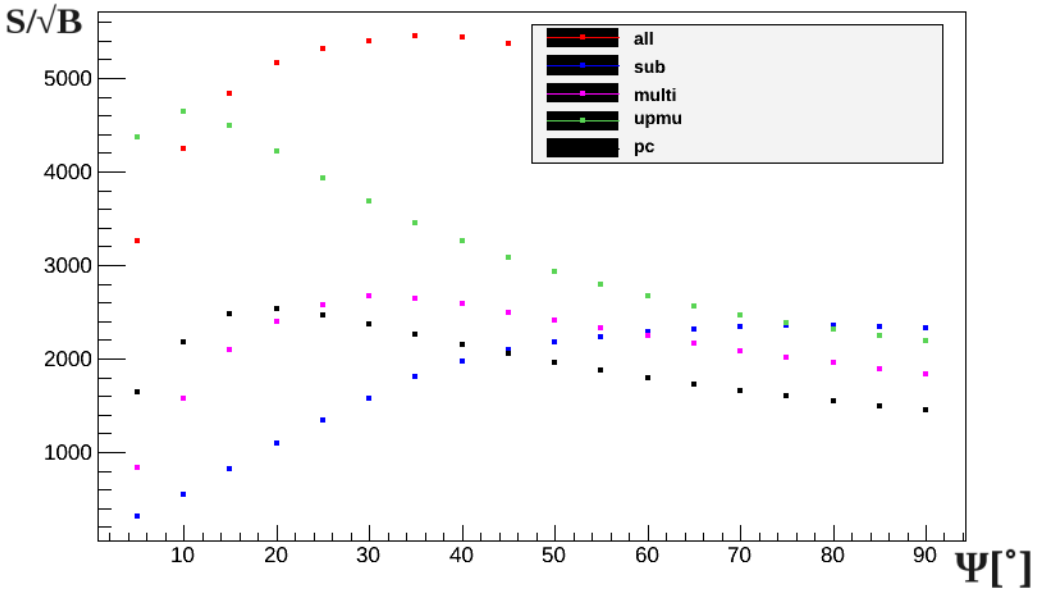

Figure 6.9: Optimization of the S/$\sqrt{B}$ ratio as a function of the angular distance from GC.

Chapter 7

Results

This chapter presents results of the searches for dark matter induced ($\nu_\mu + \bar{\nu_\mu}$) neutrino events using SK-I, II and III data sets. Search for a large-scale neutrino anisotropy using equatorial coordinate system is performed. The analysis is focused on the area of the Galactic Center (on-source) where the expected contribution from dark matter induced neutrinos should be higher than in other parts of the sky (off-source).

7.1 Upper Limits on Dark Matter Induced Neutrinos

The comparison between number of observed ($\nu_\mu + \bar{\nu_\mu}$) events in on- and off-source regions is shown in Table 7.1. Different event classes were considered separately, and for each class, the optimal size of on-source region was determined based on the simulated dark mater induced neutrino events (see Section 6.3). These results are also plotted in Fig. 7.1, where different colors indicate the average energy range for a given class. No excess of events has been observed. This is the main result of the performed analysis, which can be further interpreted under the assumptions of various DM halo models.

Table 7.1: The number of ($\nu_\mu + \bar{\nu_\mu}$) events observed in on-source and corresponding off-source regions for each considered event classes. The optimal size of the on-source region was determined separately for each class. The last column shows the upper 90% Confidence Level (C.L) limit on the allowed difference in number of signal events between two considered regions.

Sample	Size [$^\circ$]	On-source	Off-source	ΔN_{sig}	90% CL ΔN_{sig}
FC SubGeV	80	2437	2417	20$\pm$69.7	127.6
FC MultiGeV	30	155	163	-8$\pm$17.8	24.9
PC	20	59	61	-2$\pm$10.9	16.8
UPMU	10	31.8*	44.9*	-13$\pm$8.7	8.5

* In case of UPMU samples, estimated rate of bkg events due to horizontal cosmic ray muons is subtracted from the final data set.

Based on the null results in the considered samples (corresponding to various E_ν), one can derive the upper limit on the number of dark matter induced neutrinos. In the last column of Tab. 7.1, the 90% C.L. limit on the allowed difference in number of signal events is calculated using the Bayesian approach (see [46] for detailed description).

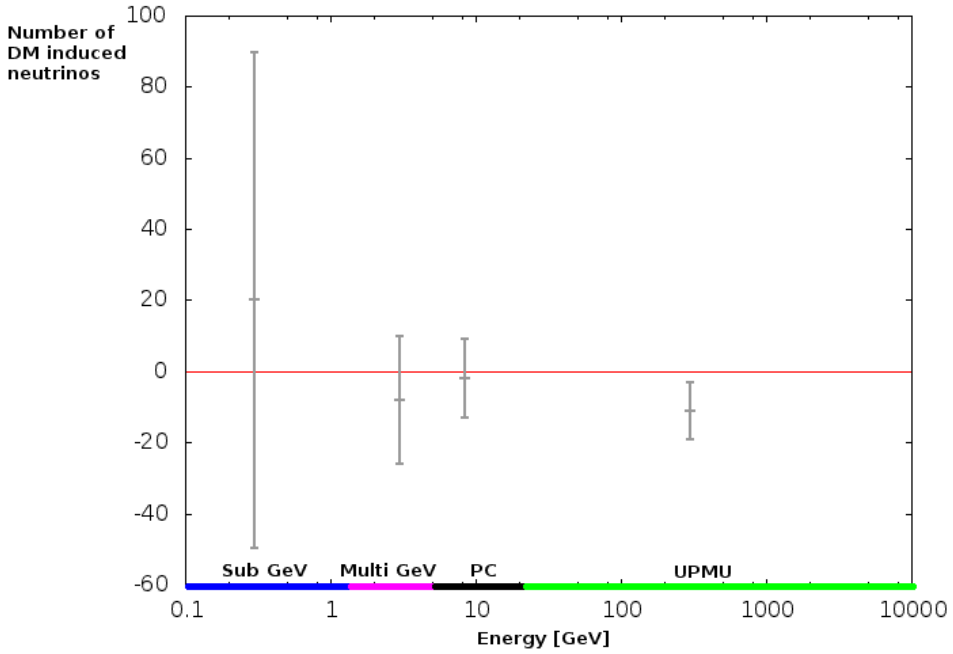

Figure 7.1: The difference in number of dark matter induced neutrinos between on-source and off-source region with statistical uncertainty, obtained for different event classes.

7.2 Upper Limits on Dark Matter Induced $(\nu_\mu + \bar{\nu}_\mu)$ Neutrino Flux

At this point one can try to interpret obtained results in terms of limits on dark matter induced neutrino flux and dark matter self annihilation cross section, taking into account given halo model. It is possible to translate upper limit on a difference in number of dark matter induced neutrinos $\Delta N^{sig}_{90\%}$ to corresponding difference in average DM-induced neutrino fluxes between on-source ($\frac{d\Phi_{\Delta\Omega_{on}}}{dE}$) and off-source ($\frac{d\Phi_{\Delta\Omega_{off}}}{dE}$) regions:

$$\Delta N^{sig}_{90\%} \rightarrow \frac{d\Phi_{\Delta\Omega_{on}}}{dE} - \frac{d\Phi_{\Delta\Omega_{off}}}{dE}. \tag{7.1}$$

Using atmospheric ν Monte Carlo, one can match the number of observed atmospheric events N_{atm} with corresponding true value of neutrino flux $\frac{d\Phi_{atm}}{dE}$ for a given neutrino energy. The same relation can be obtained for signal events. The ratio of upper limit on number of DM-induced events to the upper limit on corresponding difference in fluxes between on-source and off-source region should be the same as similar ratio for atmospheric neutrinos. Thus, from the following proportion one can derive the upper limit on a difference of fluxes of signal events in the investigated region of the sky ($\Delta\Omega = \Delta\Omega_{on} = \Delta\Omega_{off}$):

$$\frac{d\Phi_{\Delta\Omega_{on}}}{dE} - \frac{d\Phi_{\Delta\Omega_{off}}}{dE} = \frac{4\pi}{\Delta\Omega}\frac{\Delta N^{sig}_{90\%}}{N_{atm}} \cdot \frac{d\Phi_{atm}}{dE} \cdot \frac{livetime(atm)}{livetime(dst)}, \tag{7.2}$$

where one takes into account the scaling for the adopted size of on-source region ($\frac{4\pi}{\Delta\Omega}$) and the different livetime for data (dst) and atmospheric Monte Carlo (atm).

7.3 Upper Limit on Dark Matter Self-Annihilation Cross Section

Based on theoretical expectations about dark matter halo model (see Sec. 5.2), on can translate the limit on the dark matter induced neutrino flux (obtained for different event classes) into the upper limit for velocity-averaged self-annihilation cross-section $< \sigma_A v >$. In this case, Eq. 5.5 can be rewriten in the form:

$$\frac{d\Phi_{\Delta\Omega_{on}}}{dE} - \frac{d\Phi_{\Delta\Omega_{off}}}{dE} = \frac{< \sigma_A v >}{2} (J_{\Delta\Omega_{on}} - J_{\Delta\Omega_{off}}) \frac{R_{sc}\rho_{sc}^2}{4\pi m_\chi^2} \frac{dN}{dE}. \tag{7.3}$$

Using the limit for each class one can determine the corresponding limit on cross section for assumed mass of dark matter particle. These results for NFW profile are presented in Fig. 7.2. The event classes used to determine the limit for a given energy range, are plotted with different colors. The red line correspond to limit obtained in independent analysis of Super-Kamiokande data by Piotr Mijakowski[47]. This independent analysis relies on a fit of simulated dark matter signal and atmospheric neutrino background to the same data sample. The fit is repeated for various assumed dark matter masses and everytime is based on all SK data samples (FC, PC, UPMU) including e-like and μ-like sets as well.

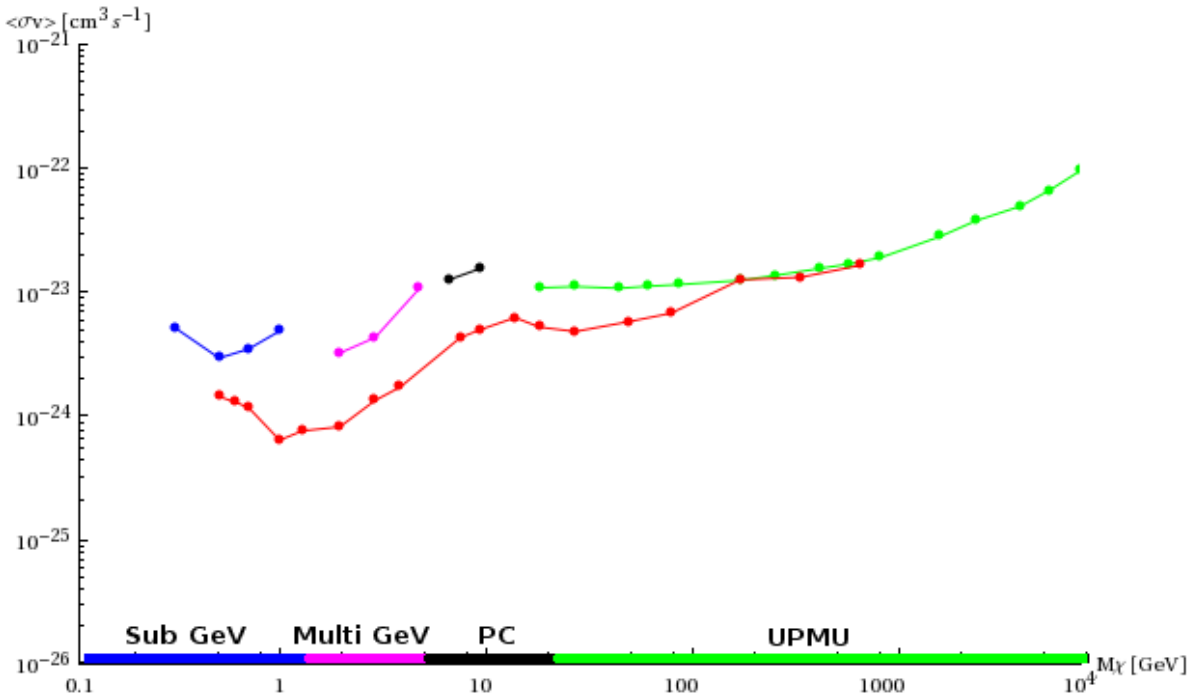

Figure 7.2: The upper 90% C.L. limit on DM self-annihilation cross section for the NFW profile (coloured line) and the limit obtained in independent analysis of the same data by Piotr Mijakowski (red line).

The upper limit for dark matter self-annihilation cross section, can be evaluated also for Moore and Kravtsov profiles, using different average signal intensities $J_{\Delta\Omega}$ (Section 5.2). The results for three considered profiles are presented in Fig. 7.3. The derived constraints on the value of $< \sigma_A v >$ strongly depend on adopted halo model. Obtained differences between benchmark model (NFW) and models used as extreme cases (Moore and Kravtsov) can reach the order of magnitude. If the size of an on-source region is smaller, the difference between obtained limits is greater due to huge discrepancies in the expected intensity of considered profiles close to Galactic Center.

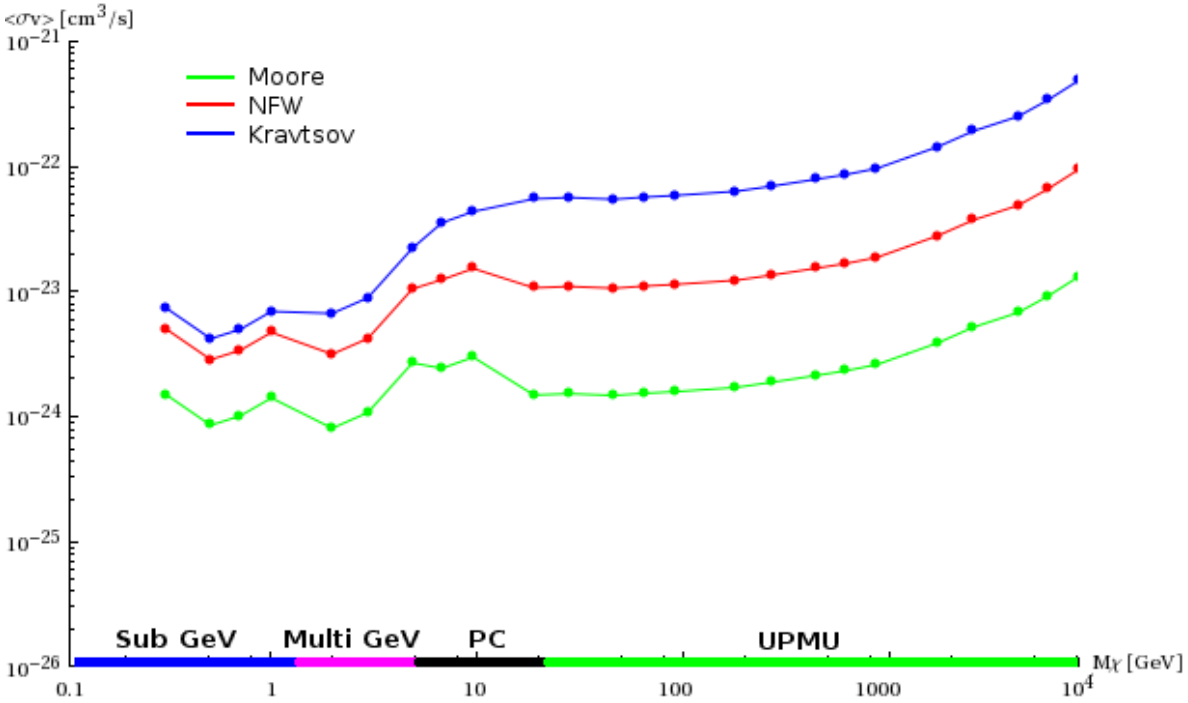

Figure 7.3: The upper 90% C.L. limit on DM self-annihilation cross section for NFW (red line), Moore (green line) and Kravtsov (blue line) profiles.

7.4 Upward Through-Going Showering Muons

Additionally, to the analysis described above one can focus only on the subsample of UPMU showering muons and derive constraints on dark matter self-annihilation cross section $< \sigma_A v >$ based on that single group of events. The average energy for these events is above 1 TeV. The estimated angular resolution of upward showering muon events is about 1.4°, which makes this sample excellent for astrophysical studies. The distribution of upward showering muons in equatorial coordinate system are shown in Fig. 7.4.

One can repeat the same on-/off- source analysis using only upward showering events. These searches can be performed in the cone only up to 5° around the GC, due to very good angular resolution of these events. The comparison between number of observed events in on- and

off-source regions and obtained limits for showering events are shown in Table 7.2. Since there is no statistically significant excess in the search cone, there is no evidence for dark matter induced upward showering muons in analysed data. In this case, one can derive the upper limits on dark matter self-annihilation cross section, as it is shown in previous section. The results obtained for NFW profile are presented in Fig. 7.5. The significant improvement in the resulting limit is visible.

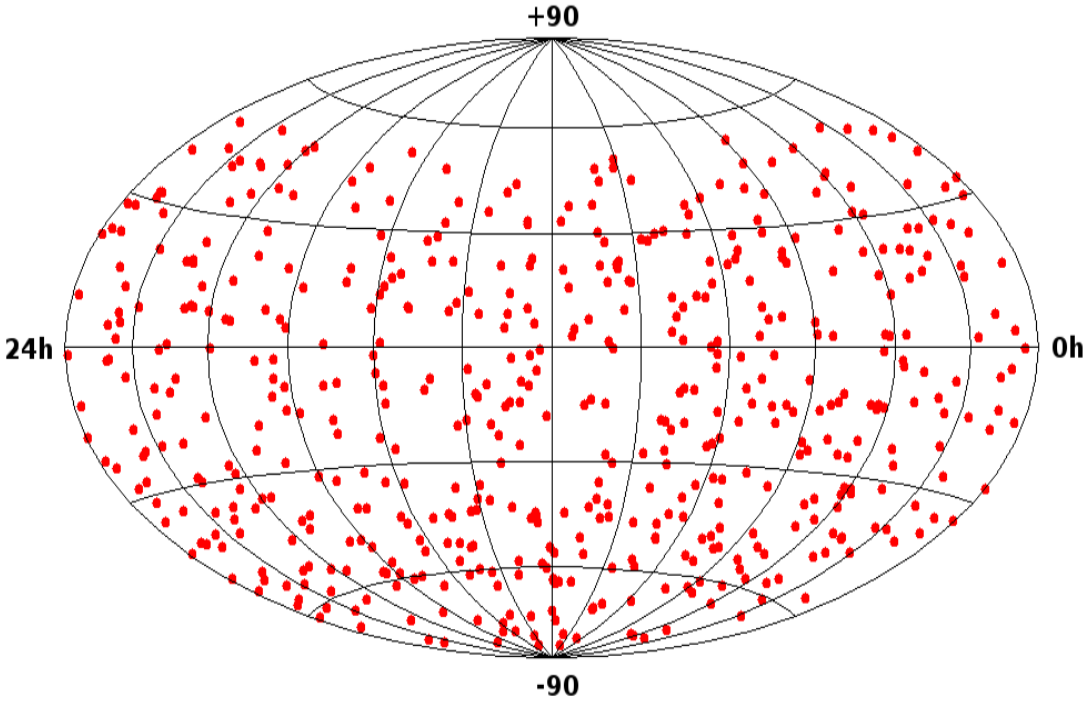

Figure 7.4: Equatorial coordinate distribution of upward showering muons from SK-I, II and III data sets.

Table 7.2: The number of events observed in on-source and corresponding off-source regions for upward showering muons. The last column shows the upper 90% C.L. limit on the allowed difference in number of signal events between two considered regions.

Size [°]	On-source	Off-source	ΔN_{sig}	σ	90% CL ΔN_{sig}
R=5	1.6*	2.0*	-0.4	1.9	2.9

* In case of UPMU samples, estimated rate of bkg events due to horizontal cosmic ray muons is subtracted from the final data set.

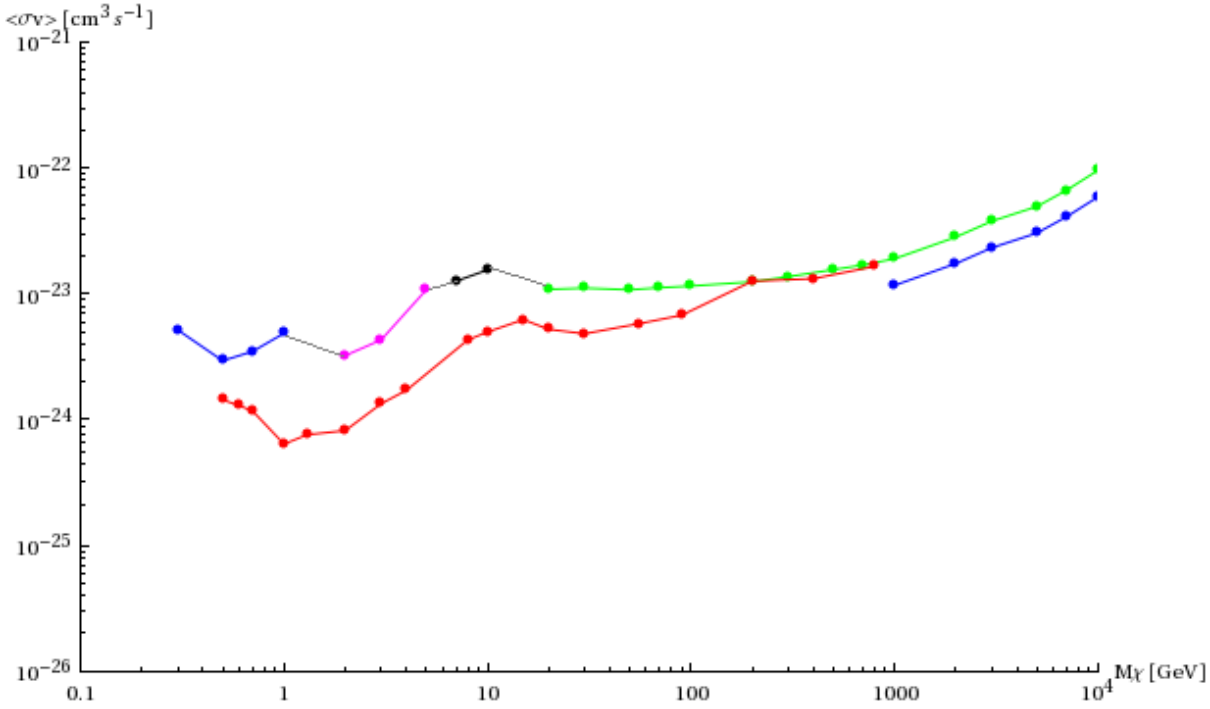

Figure 7.5: The upper 90% C.L. limit on DM self-annihilation cross section for the NFW profile (coloured line) and the limit obtained using only upward showering muons (blue line) for the highest considered WIMP masses.

Chapter 8

Summary and Conclusions

Self-annihilating or decaying dark matter in our Galaxy might produce high energy neutrinos. This would manifest in a large-scale anisotropy of observed neutrino flux. The excess of dark matter induced neutrinos is expected from the direction of the Galactic Center due to increased dark matter density in this region. It is convenient to search for this effect in equatorial coordinate system as the position of the GC is fixed in those coordinates. The direction and energy spectrum of neutrinos produced in dark matter annihilation/decay remains unchanged during neutrino propagation through the Universe. If one would be able to detect them and effectively recognize from the background of atmospheric neutrinos, they can be a powerful tool in dark matter searches.

In this thesis, the data from Super-Kamiokande detector collected between 1996-2008 has been used to search for a neutrino anisotropy expected from dark matter annihilation in the Milky Way. Three dark matter halo models were considered in the analysis: NFW, Moore and Kravtsov. A convenient tool to calculate the expected neutrino intensity for various profiles has been created. Based on atmospheric neutrino Monte Carlo and theoretical models, the simulation of dark matter induced neutrinos has been conducted. Results of simulations (Section 6.4) showed the validity of adopted method and allowed to determine the optimal conditions for performed analysis. The on/off-source method of analysis allowed for estimation of the background without necessity to use Monte Carlo events. In this way, one can avoid dependency on Monte Carlo simulations and related systematic uncertainties.

The expected anisotropy in neutrino flux has not been observed. Based on a null contribution of DM-induced neutrinos, the upper limit on a difference in signal events were obtained for on- and off- source regions. These results have been translated into upper limits for dark matter velocity-averaged self-annihilation cross section for various WIMP masses in range 300 MeV-10 TeV, assuming annihilation directly to $\nu\bar{\nu}$ pairs. This translation has been made for three considered dark matter halo models.

The analysis presented in this thesis can be continued and extended in the future. The other annihilation channels can be investigated and also the case of decaying dark matter can be considered using the same analysis method. Analysed data can also be extended by SK-IV data set, which consists of data collected after 2008 and contains a high statistic of neutrino interaction events (currently 1417.4 live days). The tools developed for the purpose of this analysis can be

used in the future studies.

The analysis methods presented in this thesis allowed to cross check results of another search for dark matter induced neutrinos which is being performed at Super-Kamiokande by Piotr Mijakowski. The two searches yield consistent results. The searches for dark matter from the Galactic Center are also complementary to other DM analyses conducted at Super-Kamiokande, like searches for dark matter induced neutrinos from the center of the Earth and from the Sun[33].

The searches for dark matter induced neutrinos are a part of global ongoing efforts to detect products of dark matter annihilation/decay in the cosmic space, such as photons or antimatter. It is very important to verify the excess in positron fraction seen by PAMELA, FERMI and AMS-02 experiments, which may be explained by dark matter annihilation, using observations of other annihilation products, such as neutrinos. The results from direct detection experiments also require independent confirmation.

Dark matter search is a highly challenging field, encompassing very different experimental techniques and detection methods. The existing results, which are not conclusive, demonstrate the importance of a multi-messenger approach to dark matter searches and validate the interest in a neutrino channel.

Bibliography

[1] J. Einasto, "Dark Matter", Astronomy and Astrophysics (2010), arXiv:0901.0632.

[2] F. Zwicky, "Spectral displacement of extra galactic nebulae", Helv. Phys. Acta. **6**, 110-127 (1933).

[3] S. Smith, "The Mass of the Virgo Cluster", Astrophysical Journal, **83**, 23-30 (1936).

[4] V. Rubin, W. Ford, "Rotation of the Andromeda Nebula from a Spectroscopic Survey of Emission Regions", Astrophysical Journal, **159**, 379-403 (1970).

[5] M. Milgrom, "A modification of the Newtonian dynamics as a possible alternative to the hidden mass hypothesis", Astrophysical Journal, **270**, 371–389 (1983).

[6] D. Clowe *et al.*, "A direct empirical proof of the existence of dark matter", Ap. J. L **648**, 109 (2006), arXiv:astro-ph/0608407.

[7] D. Larson *et al.*, "Seven-Year Wilkinson Microwave Anisotropy Probe (WMAP) Observations: Power Spectra and WMAP-Derived Parameters", Astrophys. J. Suppl. **192**, 16 (2011), arXiv:astro-ph.CO/1001.4635.

[8] Planck Collaboration: P. Ade *et al.*, "Planck 2013 results. I. Overview of products and scientific results", Astronomy and Astrophysics (2013), arXiv:1303.5062.

[9] V. Springel *et al.*, "Simulations of the formation, evolution and clustering of galaxies and quasars", Nature **435**, 629–636 (2005).

[10] K. Freese, B. Fields, D. Graff, "Death of Stellar Baryonic Dark Matter Candidates" (2000), arXiv:astro-ph/0007444.

[11] G. Jungman, M. Kamionkowski, K. Griest, "Supersymmetric dark matter", Physics Reports **267**, 195-373 (1996).

[12] L. J. Rosenberg, K. van Bibber, "Searches for invisible axions", Phys. Rept. **325** , 1 (2000).

[13] G. Servant, T. Tait, "Is the Lightest Kaluza-Klein Particle a Viable Dark Matter Candidate?", Nucl. Phys. B **650**, 391-419 (2003).

[14] H. Yuksel *et al.*, "Neutrino Constraints on the Dark Matter Total Annihilation Cross Section", Phys. Rev. D **76**, 123506 (2007), arXiv:astro-ph/0707.0196.

[15] R. Agnese *et al.* (CDMS Collaboration), "Dark Matter Search Results Using the Silicon Detectors of CDMS II" (2013), arXiv:astro-ph/1304.4279.

[16] G. Angloher *et al.*, "Results from 730 kg days of the CRESST-II Dark Matter Search", European Phys. J. C **72**, 4 (2012).

[17] E. Armengaud *et al.*, "First results of the EDELWEISS-II WIMP search using Ge cryogenic detectors with interleaved electrodes", Phys. Lett. B **687** 294-298 (2010), arXiv:0912.0805.

[18] D. Akimov *et al.*, "WIMP-nucleon cross-section results from the second science run of ZEPLIN-III", Phys. Lett. B **709** 14 (2012), arXiv:1110.4769.

[19] E. Aprile *et al.* (XENON Collaboration), "Dark Matter Results from 225 Live Days of XENON100 Data" (2012), arXiv:1207.5988.

[20] C.Amsler *et al.* (ArDM Collaboration), "The ArDM experiment" (2010), arXiv:1006.5335.

[21] R. Bernabei *et al.* (The DAMA Collaboration), "Dark Matter particles in the galactic halo: results and implications from DAMA/NaI", Int. J. Mod. Phys. D **13**, 2127-2160 (2004), arXiv:astro-ph/0501412.

[22] C. Aalseth *et al.* (The CoGeNT Collaboration), "Results from a Search for Light-Mass Dark Matter with a P-type Point Contact Germanium Detector" (2010), arXiv:astro-ph.CO/1002.4703.

[23] M. Ackermann *et al.*, "Constraints on the Galactic Halo Dark Matter from Fermi-LAT Diffuse Measurements" , Astrophysical Journal **761**, 91 (2012), arXiv:1205.6474.

[24] O. Adriani *et al.*, "The cosmic-ray positron energy spectrum measured by PAMELA", Phys. Rev. Lett. **111**, 081102 (2013), arXiv:1308.0133.

[25] AMS Collaboration, "First Results from the Alpha Magnetic Spectrometer (AMS) Experiment" (2013), http://www.ams02.org/2013/04/first-results-from-the-alpha-magnetic-spectrometer-ams-experiment/

[26] J. Chang *et al.*, "An excess of cosmic ray electrons at energies of 300–800 GeV", Nature **456**, 362-365 (2008).

[27] S. Barwick *et al.*, (The HEAT Collaboration), "Measurementsof the Cosmic-Ray Positron Fraction From 1 to 50GeV", Astrophys. J. 482, L191 (1997), arXiv:astro-ph/9703192.

[28] J. Aleksic *et al.* (MAGIC Collaboration), "Searches for Dark Matter annihilation signatures in the Segue 1 satellite galaxy with the MAGIC-I telescope" (2011), arXiv:1103.0477.

[29] A. Abramowski *et al.* (H.E.S.S. collaboration), "Search for photon line-like signatures from Dark Matter annihilations with H.E.S.S", Phys. Rev. Lett. **110** (2013) 041301.

[30] R. Wagner *et al.* (VERITAS Collaboration), "Indirect Dark Matter Searches with VERITAS" (2009), arXiv:0910.4563.

[31] R. Abbasi *et al.* (IceCube Collaboration), "Search for Dark Matter from the Galactic Halo with the IceCube Neutrino Observatory", Phys.Rev. D **84**, 022004 (2011), arXiv:astro-ph/1101.3349.

[32] S. Adrian-Martinez *et al.*, "Search for cosmic neutrino point sources with four year data of the ANTARES telescope" (2012) Astrophysical Journal **760** 53, arXiv:1207.3105.

[33] R. Kappl, M. Winkler, "New Limits on Dark Matter from Super-Kamiokande" (2011), Nucl. Phys. B **850**, 505-521.

[34] S. Fukuda *et al.* (The Super-Kamiokande Collaboration), "The Super-Kamiokande detector", Nucl. Instruments and Methods A **501**, 418-462 (2003).

[35] Y. Fukuda *et al.* (The Super-Kamiokande Collaboration), "Evidence for oscillation of atmospheric neutrinos", Phys. Rev. Lett. **81**, 1562-1567 (1998), arXiv:hep-ex/9807003.

[36] J. Hosaka *et al.* (The Super-Kamkiokande Collaboration), "Solar neutrino measurements in Super-Kamiokande-I", Phys. Rev. D **73**, 112001 (2006), arXiv:hep-ex/0508053.

[37] Y. Hayato *et al.* (The T2K Collaboration), "Letter of Intent: Neutrino Oscillation Experiment at JHF", http://neutrino.kek.jp/jhfnu/loi/loi.v2.030528.pdf.

[38] J. Diemand, M. Kuhlen, P. Madau, "Formation and evolution of galaxy dark matter halos and their substructure", Astrophysical Journal **667**, 859 (2007), arXiv:astro-ph/0703337.

[39] B. Menard *et al.*, "Measuring the galaxy-mass and galaxy-dust correlations through magnification and reddening", Mon. Not. Roy. Astron. Soc. **405**, 1025 (2010), arXiv::astro-ph/0902.4240.

[40] J. Navarro, C. Frenk, S. White, "The Structure of Cold Dark Matter Halos", Astrophysical Journal **462**, 563 (1996), arXiv:astro-ph/9508025.

[41] B. Moore *et al.*, "Cold collapse and the core catastrophe", Mon. Not. Roy. Astron. Soc. **310**, 1147 (1999), arXiv:astro-ph/9903164.

[42] A. Kravtsov *et al.*, "The Cores of Dark Matter-dominated Galaxies: Theory versus Observations", Astrophysical Journal **502**, 48 (1998), arXiv:astro-ph/9708176.

[43] http://www.wolfram.com/mathematica/

[44] Y. Ashie *et al.* (The Super-Kamiokande Collaboration), "A Measurement of Atmospheric Neutrino Oscillation Parameters by SuperKamiokande I", Phys. Rev. Lett. D **71**, 112005 (2005), arXiv:hep-ex/0501064.

[45] http://www.thienvanhoc.org/

[46] R. Barnett *et al.* (The Particle Data Group), "Review of Particle Physics", Physical Review D **54**, 164 (1996).

[47] P. Mijakowski, "Direct and Indirect Search for Dark Matter", Ph.D. thesis, Andrzej Sołtan Institute for Nuclear Studies (2011).

[48] S. Desai *et al.* (The Super-Kamiokande Collaboration), "Study of TeV Neutrinos with Upward Showering Muons in Super-Kamiokande", Astropart. Phys. **29**, 42 (2008), hep-ex/arXiv:0711.0053v1.